

Combined effects of composite thermal energy storage and magnetic field to enhance productivity in solar desalination

Dsilva Winfred Rufuss, D.; Arulvel, S.; Anil Kumar, V.; Davies, P.A.; Arunkumar, T.; Sathyamurthy, Ravishankar; Kabeel, A.e.; Anand Vishwanath, M.; Sai Charan Reddy, D.; Dutta, Amandeep; Agrawal, Mayank; Vilas Hiwarkar, Vedant

DOI:

[10.1016/j.renene.2021.07.124](https://doi.org/10.1016/j.renene.2021.07.124)

License:

Creative Commons: Attribution-NonCommercial-NoDerivs (CC BY-NC-ND)

Document Version

Peer reviewed version

Citation for published version (Harvard):

Dsilva Winfred Rufuss, D, Arulvel, S, Anil Kumar, V, Davies, PA, Arunkumar, T, Sathyamurthy, R, Kabeel, AE, Anand Vishwanath, M, Sai Charan Reddy, D, Dutta, A, Agrawal, M & Vilas Hiwarkar, V 2021, 'Combined effects of composite thermal energy storage and magnetic field to enhance productivity in solar desalination', *Renewable Energy*, vol. 181, pp. 219-234. <https://doi.org/10.1016/j.renene.2021.07.124>

[Link to publication on Research at Birmingham portal](#)

General rights

Unless a licence is specified above, all rights (including copyright and moral rights) in this document are retained by the authors and/or the copyright holders. The express permission of the copyright holder must be obtained for any use of this material other than for purposes permitted by law.

- Users may freely distribute the URL that is used to identify this publication.
- Users may download and/or print one copy of the publication from the University of Birmingham research portal for the purpose of private study or non-commercial research.
- User may use extracts from the document in line with the concept of 'fair dealing' under the Copyright, Designs and Patents Act 1988 (?)
- Users may not further distribute the material nor use it for the purposes of commercial gain.

Where a licence is displayed above, please note the terms and conditions of the licence govern your use of this document.

When citing, please reference the published version.

Take down policy

While the University of Birmingham exercises care and attention in making items available there are rare occasions when an item has been uploaded in error or has been deemed to be commercially or otherwise sensitive.

If you believe that this is the case for this document, please contact UBIRA@lists.bham.ac.uk providing details and we will remove access to the work immediately and investigate.

1 **Combined effects of composite thermal energy storage and magnetic field to enhance**
2 **productivity in solar desalination**

3 D. Dsilva Winfred Rufuss^{1,2*}, S. Arulvel¹, V. Anil Kumar¹, P.A. Davies², T. Arunkumar³,
4 Ravishankar Sathyamurthy^{4,5}, A.E. Kabeel⁵, M. Anand Vishwanath¹, D. Sai Charan Reddy¹,
5 Amandeep Dutta¹, Mayank Agrawal¹, Vedant Vilas Hiwarkar¹

6 ¹School of Mechanical Engineering, Vellore Institute of Technology (VIT), Vellore-632014,
7 Tamil Nadu, India

8 ²School of Engineering, University of Birmingham, Edgbaston, Birmingham B15 2TT, UK

9 ³National Center for International Research on Photoelectric and Energy Materials, Yunnan
10 Province Engineering Research Center of Photocatalytic Treatment of Industrial Wastewater,
11 School of Chemical Sciences and Technology, Yunnan University, Kunming-650091, China

12 ⁴Department of Mechanical Engineering, KPR Institute of Engineering and Technology,
13 Coimbatore, Tamil Nadu, India

14 ⁵Mechanical Power Engineering Department, Faculty of Engineering, Tanta University, Tanta,
15 Egypt

16 **Abstract**

17 The conventional solar still is limited to a daily yield of approximately 2 – 3.5 kg/m²/day. To
18 increase the yield, this study investigates experimentally the combined effects of latent and
19 sensible energy storage together with magnetization. Paraffin and novel high-thermal
20 conductivity nanomaterial (graphite plate) were used as latent and sensible heat storage
21 materials, respectively. There was an overall increase of 62% and 235% in the daytime and
22 night-time yield, respectively, giving a total yield of 5.5 kg/m²/day compared to 3.4 kg/m²/day
23 for a conventional still. Enviro-economic parameters like emissions, CO₂ mitigation and carbon
24 credit (CC) earned were also investigated. Energy matrices analysis and water quality checks
25 were performed to estimate the energy-payback time, life cycle conversion efficiency (LCCE)
26 and purity of desalinated water. The cost per liter of freshwater was found to be 3.7% cheaper
27 than for a conventional still and 69% cheaper than bottled water in India. Over a 30 year period,
28 40.3 Tonnes of CO₂ will be mitigated contributing a CC and LCCE of \$402 and 0.52,
29 respectively. The proposed modified still is recommended as a substitute for conventional stills
30 and stills with simple energy storage.

31 *Keywords:* composite thermal energy storage; graphite plate-paraffin; modified still; ferrite
32 magnets; techno-enviro-economical; productivity.

*Corresponding author: D. Dsilva Winfred Rufuss *E-mail address:* dsilva.kongu@gmail.com

Nomenclature

AC	annual cost (\$)
AMC	annual maintenance and operational cost(\$)
ASV	annual salvage value (\$)
BIS	bureau of Indian standards
CC	carbon credit earned (\$)
CNT	carbon nanotube
CO ₂	carbon dioxide
CPL	cost per liter (\$)
CRF	capital recovery factor
CuO	copper oxide
DO	dissolved oxygen (%)
DSC	Differential scanning calorimeter
FAC	fixed annual cost (\$)
GDP	Gross Domestic Product
GO	graphene oxide
LCCE	life cycle conversion efficiency
M	annual productivity (kg/m ²)
N	number of days
NO	nitric oxide
P	present capital cost (\$)
PCM	phase change material
pH	parts of hydrogen
Ppm	parts per million
PVC	Polyvinyl chloride
R&D	research and development
S	salvage value (\$)
SAS	School of Advanced Sciences
SFF	sinking fund factor
SO ₂	sulphur dioxide
Ta	ambient temperature (°C)
TDS	total dissolved solids (mg/L)
TES	thermal energy storage
Tgraphite	temperature of graphite plate (°C)
Tg	temperature of glass (°C)
TiO ₂	titanium dioxide
Tpcm	temperature of phase change material (°C)
Tw	water temperature (°C)
USD	United States dollar (\$)
VIT	Vellore Institute of Technology
Y	Total years of operation

34

35

36

37 **1. Introduction**

38 Freshwater is one of the basic requirements of all living creatures on the earth. Even though
39 73% of the earth is covered with water, only 3% is freshwater. The total freshwater available
40 for usage is estimated to be 0.36% [1,2]. Roughly one million people die each year due to lack
41 of access to good quality water [3]. Desalination technologies help to remedy this water crisis.
42 The various desalination techniques include membrane desalination technologies
43 (electrodialysis, reverse osmosis, forward osmosis) and thermal desalination technologies
44 (vapour compression evaporation, adsorption desalination, solar stills, multi-stage flash and
45 distillation) [4,5,14,6–13]. In general, membrane technologies and most of the thermal
46 desalination technologies are expensive, energy-intensive processes, as such not very feasible
47 in rural areas [15]. Among the various options, the solar still is a thermal desalination
48 technology that operates at zero fuel cost (as it is driven by solar energy) and as such one the
49 more economic technologies available [16–18].

50 The conventional solar still is limited to a low daily yield of approximately 2–3.5
51 kg/m²/day, which is insufficient for an average family [19]. Enhancing this yield is an
52 important research and development (R & D) area, wherein researchers are trying to
53 incorporate advanced techniques like solar collectors, solar photovoltaic, thermal energy
54 storage and solar pond. [20–23]. Among these, thermal energy storage is used to improve the
55 daily yield by providing freshwater even during the night [24–26].

56 Generally, thermal energy can be stored by sensible heat (without phase change) and latent
57 heat (with phase change) energy storage materials [27]. Many sensible heat energy storage
58 materials (Fig. 1) were used by researchers from the year 1981 to 2020, including jute cloth
59 [28], black rubber mat [29], black gravel [30], aluminium plates [31,32], charcoal granules
60 [33], packed glass ball [34], granite [35], sponges [36,37], fins [38], sand [39], black rocks
61 [40], dried sand [41], vertical jute cloth [42], dry cow dung [43], thermic fluid [44,45], bamboo
62 cotton [46], marble pieces [47] and fins [48]. In recent years (i.e. 2018 and 2019), research was
63 carried using novel materials and combining more than one materials [49], [50], [51], [52],
64 [53], [54], [55], [56] to enhance the productivity. A detailed comparison of productivity
65 enhancement using these various materials is shown in Table. 1. It is evident that the sensible
66 heat energy storage materials gave a significant productivity improvement. However, emerging
67 high-thermal conductivity energy storage materials such as CNT and graphite plates (in the
68 bulk volume) have not yet been incorporated and investigated in the solar still.

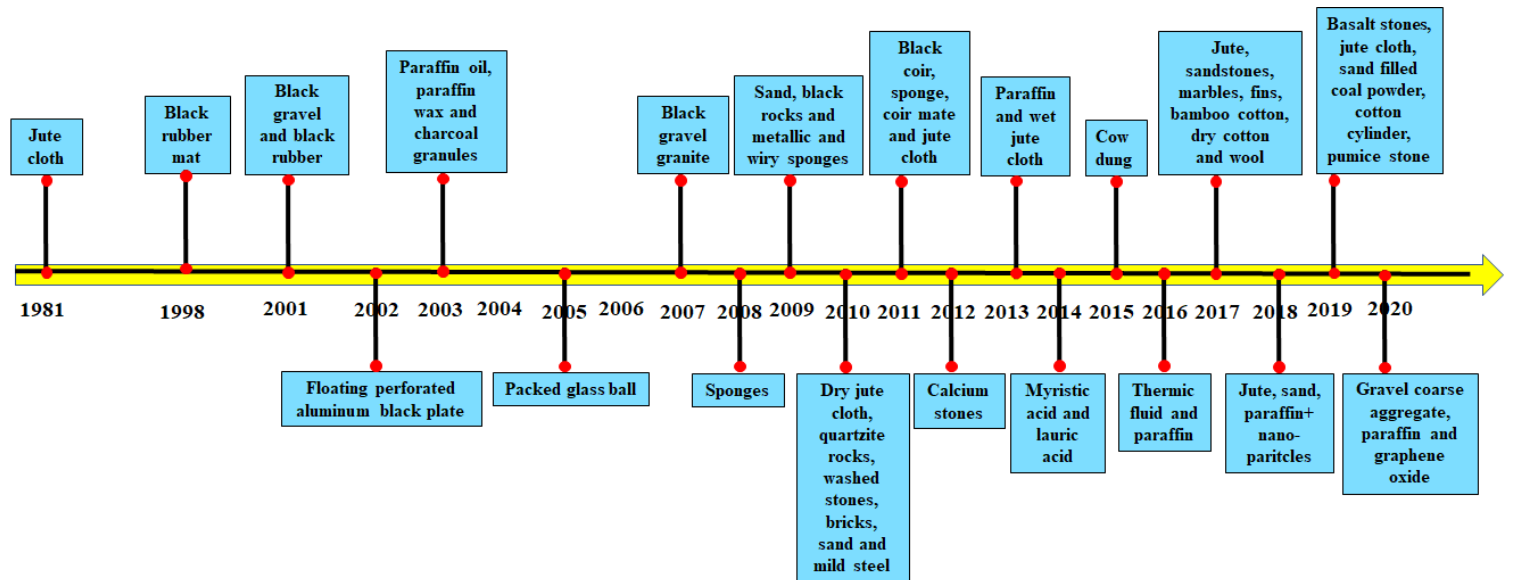


Fig. 1. Historical evolution of thermal energy storage materials in solar desalination

Unlike sensible heat energy storage, latent heat energy storage in solar still gained interest relatively recently in 2003 [57], and slowly gained momentum since then [58–62]. There are many reviews available about the integration of latent heat energy storage material in the solar still [63,64], covering various types of latent heat energy storage materials such as paraffin, lauric acid, glauber’s salt and stearic acid [24,27]. Among these, paraffin is most widely used owing to its low cost and favourable thermo-physical and chemical properties [26,63,65,66]. Up till now, studies only looked at materials used individually. Composite thermal energy storage is a new concept that combines both sensible and latent heat energy storage in the solar still. This technique was initiated in 2016 [67] and only a few studies have been reported so far.

Shalaby et al. (2016) used wick and paraffin for composite thermal energy storage and achieved a 41% improvement in yield over a conventional still [67]. Kabeel et al. (2019) used black gravel (as sensible heat energy storage material) and paraffin wax (as latent heat energy storage material) to obtain an improvement of 37% [68]. These experiments show it to be a promising technique that merits further investigation. Moreover, none of the studies investigated the integration of recently evolved high thermal conductivity sensible heat energy storage materials (like CNT and graphite) along with the latent heat energy storage materials in a solar still.

Recently (in 2019) Indian researchers found that magnetizing (through ferrite magnets) the feed water enhances the distillate yield [69]. Usually, in conventional stills, the presence of Van der Waals force between the soluble salts and water molecules increases the boiling point elevation and leads to the low vapor pressure [70–75]. Whereas the still integrated with ferrite magnets induce a magnetic field which tends to break the Van der Waals force between the

94 water molecules and soluble salts [70–75]. This phenomenon increases the diffusion coefficient
 95 of salt ions and mobility of water molecules, which in turn increase the vapor pressure and
 96 enhances the evaporation process [70–75]. The integration of magnets increases the partial
 97 pressure difference between the water and glass cover, which in turn increases the evaporative
 98 heat transfer coefficient and enhances productivity by 49% [69]. However, the combined
 99 effects of heat storage and magnetisation have yet to be investigated.

100 To summarise these findings, the following areas have not yet been investigated in solar
 101 stills: (i) new (graphite plates and CNT) sensible heat energy storage materials; (ii) combination
 102 of such materials with latent heat energy storage; (iii) magnetisation together with such
 103 composite energy storage. The current study aims to address these research gaps. Thus, the
 104 specific objectives are to: (i) analyse the productivity enhancement through composite thermal
 105 energy storage technique along with the magnetizing effect together in solar still (modified
 106 still); (ii) investigate the technical and economic feasibility of the proposed modified still, (iii)
 107 conduct an enviro-economic analysis of it; (iv) perform energy matrices analysis associated
 108 with the modified still, and (v) test the quality of water from the modified still to reassure that
 109 the desalinated water quality is within the permissible limits of the Bureau of Indian Standards
 110 (BIS).

111 **Table 1. Summary of existing literature in solar still integrated with sensible and latent heat**
 112 **energy storage materials (where data are provided)**

Sl. No	Reference	Year	Types of energy storage	Materials used	Findings
1.	[28]	1981	Sensible heat energy storage	Jute cloth	Productivity augmented by 34%
2.	[29]	1998	Sensible heat energy storage	Black rubber mat	38% increase in the productivity
3.	[30]	2001	Sensible heat energy storage	Black gravel and black rubber	20% improvement in the cumulative yield
4.	[31,32]	2002	Sensible heat energy storage	Floating perforated aluminium black plate	Yield was enhanced by 40%
5.	[33]	2003	Sensible heat energy storage	Charcoal granules	Yield was enhanced by 15%
6.	[57]	2003	Latent heat	Paraffin oil and paraffin wax	The efficiency was enhanced to 36.2%

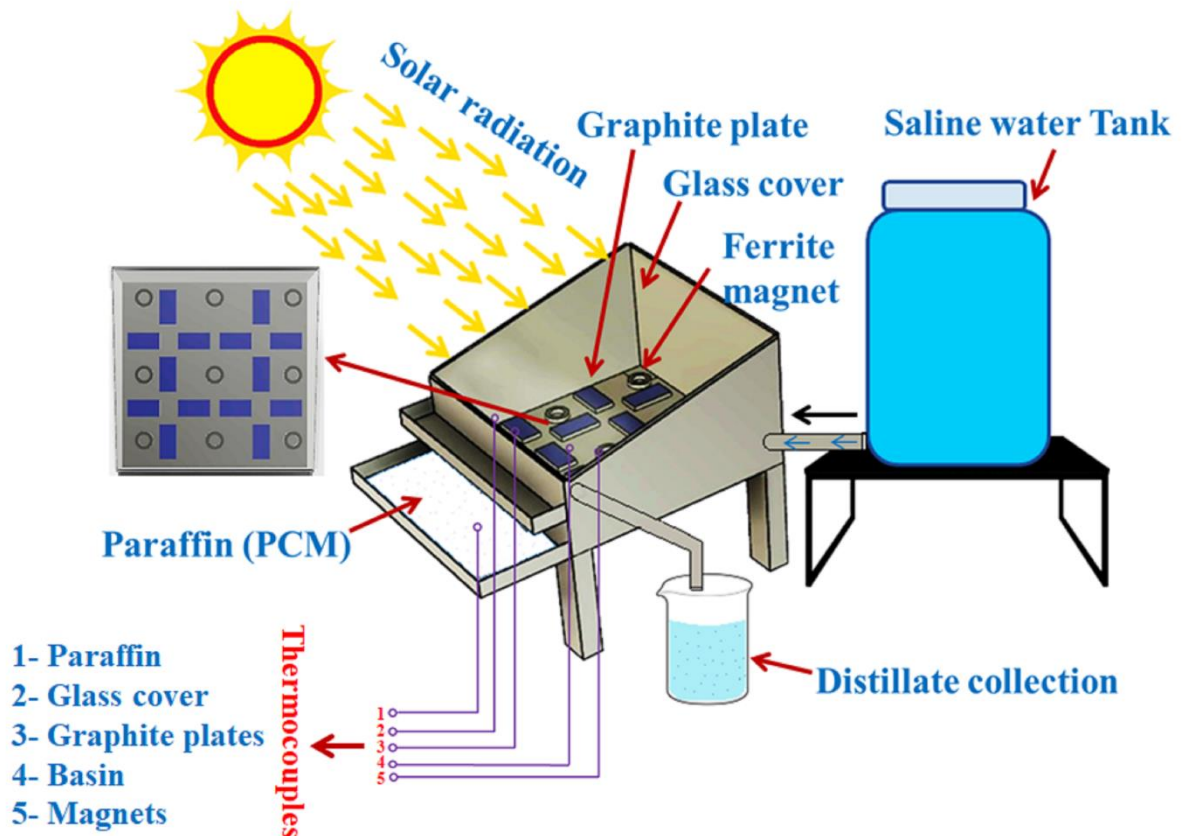
7.	[34]	2005	Sensible heat energy storage	Packed glass ball	Productivity improved by 7.5%
8.	[35]	2007	Sensible heat energy storage	Black gravel granite	Productivity improved by 20% Productivity enhanced to 3.9 kg/m ²
9.	[36–38]	2008	Sensible heat energy storage	Sponges	Productivity is 2.26 kg/m ² . 15.3% higher productivity compared to the conventional still
10.	[39]	2009	Sensible heat energy storage	Sand	23% enhancement in the productivity
11.	[40]	2009	Sensible heat energy storage	Black rocks and metallic wiry sponges	Black rocks gave better productivity as compared to wiry sponges
12.	[41]	2010	Sensible heat energy storage	Sand	75% enhancement in the productivity
13.	[42]	2010	Sensible heat energy storage	Dry jute cloth	20% increase in the cumulative yield. Daily yield enhanced to 4 kg/m ²
14.	[25]	2010	Sensible heat energy storage	Quartzite rocks, washed stones, bricks and mild steel	Quartzite rock gave the maximum yield comparing other materials.
15.	[58]	2014	Latent heat energy storage	Myristic acid, lauric acid	Lauric acid gave better yield as compared to myristic acid
16.	[43]	2015	Sensible heat energy storage	dry cow dung	35% increase in the daily yield
17.	[44,45]	2016	Sensible heat energy storage	Salt encapsulated spherical plastic container and thermic fluid	The daily yield was enhanced by 66%
18.	[59]	2016	Latent heat energy storage	Paraffin	31% increase in the productivity
19.	[60]	2016	Latent heat energy storage	Paraffin	67.18% increase in the productivity
20.	[61]	2016	Latent heat energy storage	Paraffin	109% increase in the daily yield
21.	[62]	2016	Latent heat energy storage	Paraffin	Productivity increases by 49%. The daily yield was 2.1 kg/m ² .
22.	[67]	2016	Sensible heat and latent heat energy storage	Paraffin	Daily yield increased to 3.7 kg/m ² .
23.	[46]	2017	Sensible heat energy storage	Jute, bamboo cotton, dry cotton and wool	Bamboo cotton yielded better results with 51.9% higher yield

24. [47]	2017	Sensible heat energy storage	Sandstones, marble pieces	Sandstones gave higher productivity as compared to marbles
25. [48]	2017	Sensible heat energy storage	Fins along with condensers	41.9% improvement in the daily yield
26. [49]	2018	Sensible heat energy storage	Jute cloth and sand heat storage	15% improvement in the yield
27. [50]	2018	Sensible heat energy storage	Absorber tube coated with graphite	80% improvement on the cumulative yield
28. [27]	2018	Latent heat energy storage	Paraffin+CuO, Paraffin+TiO ₂ , Paraffin+GO	Paraffin with titanium oxide gave better productivity of 5.28 kg/m ² compared to the GO and CuO
29. [51]	2019	Sensible heat energy storage	Sand-filled coal powder and cotton cylinder	Yield improved by 30.9%
30. [52,53]	2019	Sensible heat energy storage	Basalt stones Jute cloth	Yield improved by 33.37% Productivity enhanced by 18%
31. [54]	2019	Sensible heat energy storage	Copper oxide nanoparticles coated absorber plate and sponges	41% improvement in the daily yield
32. [55]	2019	Sensible heat energy storage	Pumice stones	Cumulative yield enhances by 28%
33. [68]	2019	Latent heat and sensible heat energy storage	Paraffin and Black gravel	Achieved daily yield of 3.27 kg/m ²
34. [56]	2020	Sensible heat energy storage	Gravel coarse aggregate	Productivity enhanced to 4.21 kg/m ²

113

114 2. System description

115 Two solar stills (conventional and modified), each of 1m² area, were fabricated using
 116 aluminium sheets and covered with a transparent glass cover of thickness 4 mm. The inclination
 117 of the cover was at 12° (equal to the latitude of the Vellore, Tamil Nadu, India, where the still
 118 was located). To reduce the heat loss from the system to the surroundings, a foam strap with
 119 epoxy glue was used to fix the glass on the top of both solar stills. The inner walls of the solar
 120 stills were coated with aluminium enamel and the base was coated with black synthetic enamel
 121 paint to enhance the absorptivity and reflectivity of solar radiation onto the system. The
 122 modified still included ferrite magnets, graphite plates and paraffin arranged as follow (Fig. 2).



123
 124 **Fig. 2. Schematic setup of modified solar still with composite energy storage and ferrite**
 125 **magnets**

126 Fourteen graphite plates (each of 150 mm × 70 mm × 25 mm), which are insoluble in
 127 water, were purchased from Triton Graphite, Gujarat, India and placed on the basin of the solar
 128 still following the pattern suggested by Dumaka et al. (2019) [69] (Fig. 3). The specifications
 129 of graphite plates are tabulated in Table 2. Ring-shaped hollow ferrite magnets of grade N42
 130 (09 numbers) each of 6 cm outer diameter and 3.2 cm inner diameter with a magnetic field
 131 strength of 90 mT were purchased from Magna Tronix, Chennai, India. The magnets were
 132 arranged geometrically as suggested in the literature to provide a uniform distribution of
 133 magnetic field strength across the basin [69,76,77]. The detailed specifications of the ferrite
 134 magnet are given in Table 3. A small reservoir of 2.5 cm height was fabricated below the basin
 135 to hold 10 kg latent heat energy storage material (paraffin). The melting and solidification
 136 characteristics of the paraffin were tested using Nano DSC differential scanning calorimeter
 137 from TA instruments in the School of Advanced Sciences (SAS), VIT University, Vellore,
 138 India. As per the recommendations given in the literature [27,78,79] suggesting that the amount
 139 of brine water should be less than the total volume of paraffin, 9 kg of saline water (tap water)
 140 was fed inside the solar still. The specifications of the paraffin used in the study are tabulated
 141 in Table 4. Experimental observations were carried out during March 2020 at the roof-top of

142 Renewable Energy Sources Laboratory-GDN block, VIT University (12.91° N, 79.13° E),
 143 Tamil Nadu, India.

144 **Table 2. Specification of graphite plates used in the present study**

Parameters	Specifications
Grade and color	1 st grade and black color
Length x bredth x thickness (mm)	150 x 70 x 25
Thermal conductivity (W/mK)	390
Temperature	up to 2000°C
Thermal expansion (µm/m-K)	4.9
Young's Modulus (GPa)	21
Ultimate tensile strength (MPa)	18
Heat of vaporization	128 k-Cal/gm atom at 4612°C

145

146 **Table 3. Thermal properties of ferrite magnet used in the modified still**

Properties	Specifications
Density (g/cm ³)	4.9 to 5.1
Thermal conductivity (W/mK)	4186.92
Electrical resistivity (ohm-cm)	106
Tensile strength (psi)	5000
Flexural strength (psi)	9000
Hardness (Mohs)	7
Curie temperature (°C)	450
Remanence (Br)	0.41-0.42
Intrinsic coercive force (Hcj)	250-260
Max. energy (kJ/m ³)	32.0-33.0

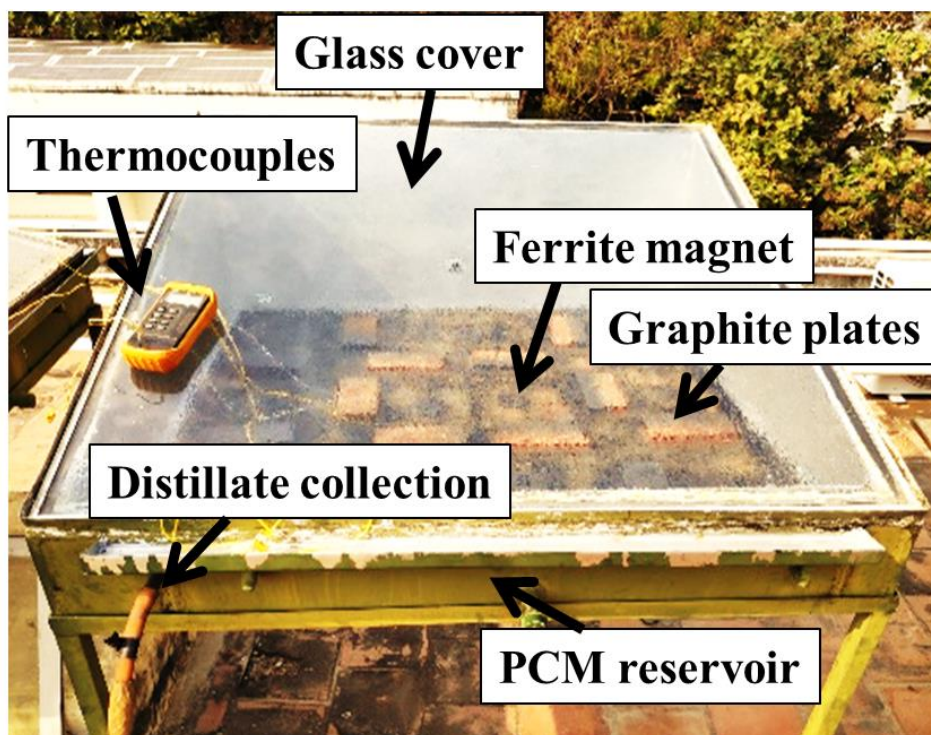
147

148 **Table 4. Properties of the phase change material (paraffin)**

Sl. No	Properties	Corresponding value
1	Melting temperature range	57-59°C
2	Density (solid/liquid)	820/770 kg/m ³
3	Specific heat (solid/liquid)	2.9/2.51 kJ/kg
4	Latent heat of fusion	285 kJ/kg
5	Thermal conductivity	0.28 W/mK

149

150 K-type (KC-PVC-K-24-180) thermocouples have been used to detect the temperatures
151 of magnets, graphite, paraffin, inner glass, ambient and water in the solar still. The tap water
152 with pH: 7.7, TDS: 330 ppm, hardness: 254 mg/L, dissolved oxygen: 78%, fluoride: 1.9 mg/L,
153 chloride: 31.4 mg/L, electrical conductivity: 637 $\mu\text{s/m}$, calcium ions: 29.7 mg/L, magnesium
154 ions: 33 mg/L, sodium ions: 372 mg/L, potassium ions: 95 mg/L and sulphate ions: 37 mg/L
155 was used as the feed water. The temperatures of the various components of the solar still were
156 observed on an hourly basis from 9:00 h to 21:00 h. A plastic graduated cylinder was used to
157 measure the distillate output. The whole system was insulated with glass wool of 30 mm
158 thickness to lessen the heat loss further. The solarimeter and anemometer were used in the
159 experiment to measure the solar intensity and wind velocity, respectively.



160
161 **Fig. 3. Experimental picture of the modified solar still showing graphite plates, ferrite magnets**
162 **and paraffin**

163 The technical details of the various measuring instruments including their range and
164 accuracy are tabulated in Table 5. To estimate the impacts of errors associated with the
165 experiments on the results and conclusions, an uncertainty analysis was carried out for the
166 experimental observation parameters such as various temperature components, hourly yield
167 and cumulative productivity, as per the procedure suggested in the literature [27,36,64,80]. The
168 internal uncertainty and the average of averages in the observations were found to be 0.0024
169 and 0.19 respectively, corresponding to an uncertainty percentage of 1.2%. The uncertainty
170 percentage of the experiment was thus found to be very low and consistent with that achieved
171 by the other researchers e.g. Kabeel et al. [68] with 6.8%, Arunkumar et al. [54] with 1.88%

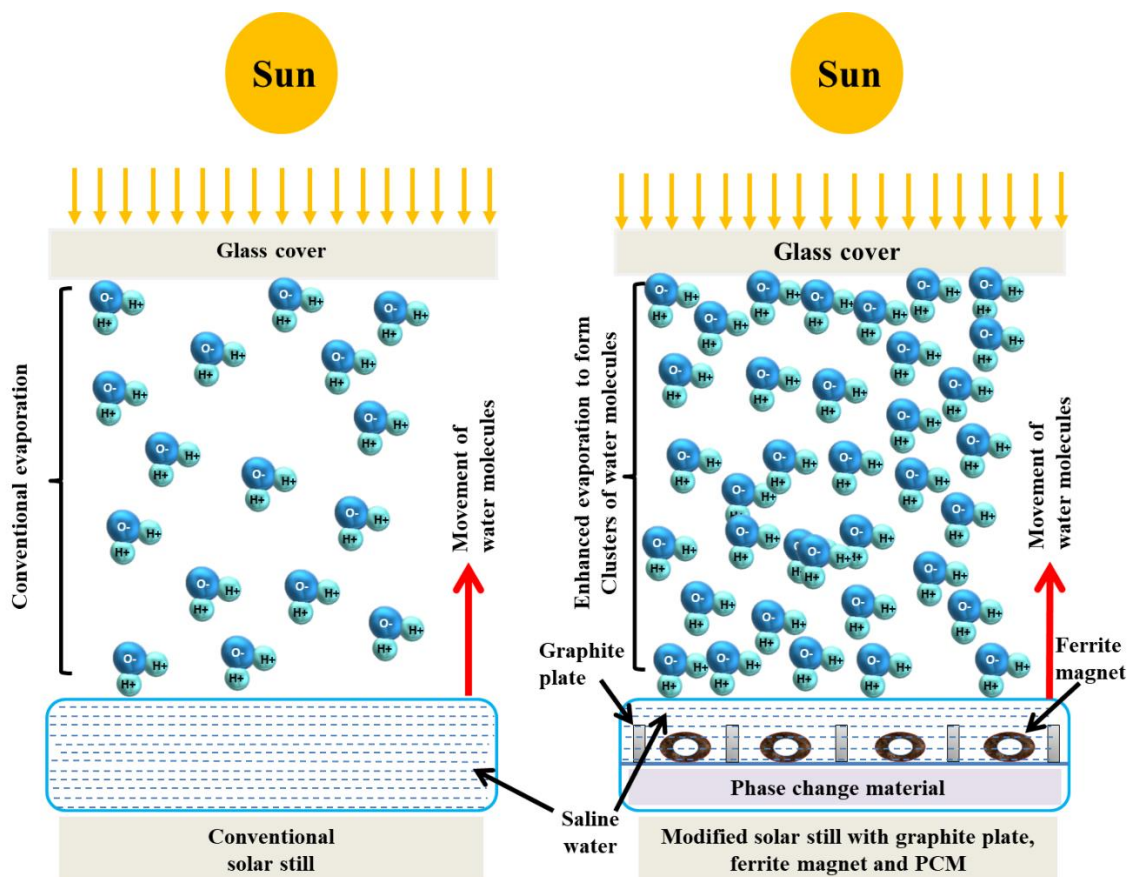
172 and Rufuss et al. [27] with 2.06%. After the experiments, the desalinated water was taken for
 173 quality testing in the Environmental and Water Resource Laboratory, VIT University, Vellore,
 174 India.

175 **Table 5. Accuracy and range measurement instruments used for the experiment**

Sl. No	Instrument	Accuracy	Range
1	Solarimeter	$\pm 2 \text{ W/m}^2$	0 – 2000 W/m^2
2	Thermocouple	$\pm 0.1 \text{ }^\circ\text{C}$	0 – 1300 $^\circ\text{C}$
3	Graduated cylinder	$\pm 1 \text{ ml}$	1000 ml
4	Gaussmeter	0.1 mG / 0.01 μT	0-2000 μT
5	Anemometer	$\pm 0.1 \text{ m/s}$	0.4-35 m/s
6	Differential scanning calorimetry (DSC)	Baseline stability $\pm 0.028 \text{ } \mu\text{Watts}$	10 $^\circ\text{C}$ to 160 $^\circ\text{C}$ with the scan rate 0.05 $^\circ\text{C}$ to 2 $^\circ\text{C/minute}$

176 **3. Working principle**

177 Fig. 4 shows the working principle of the modified still which has PCM, graphite plates
 178 and ferrite magnets.



179
 180 **Fig. 4. Working principle of modified still showing a productivity enhancement with**
 181 **graphite plates, paraffin (PCM) and ferrite magnets**

182 The addition of graphite plates increases the evaporation of water molecules from the brine
183 to the inner surface of the glass cover. The magnetization of water molecules also plays an
184 important role in the evaporation of water molecules. Generally, in saline water, the water
185 molecules adhere to the salt ions through weak Van der Waals bonding. It is important to
186 weaken the bonding between the salt ions and water molecules to increase the mobility of salt
187 ions (from salinized water to the basin) and water molecules (from the basin to the inner surface
188 of the glass cover). This can be achieved through the electric field or magnetic field [69,81]. In
189 this study, the magnetic field is preferred based on previous studies in solar desalination
190 [69,82,83]. The magnetic field is also responsible for increasing the partial pressure difference
191 between water and glass cover, which should improve the evaporation process.

192 In addition, sensible heat storage materials in solar still absorb the heat energy from the
193 sun and store them in the form of sensible heat and release the heat during the nocturnal hours
194 without changing phase. Whereas the latent heat storage material works on the same
195 mechanism as the sensible heat storage materials, except for the fact that they change their state
196 of matter from solid to molten state while they absorb the heat and vice-versa when they release
197 the heat. These materials absorb and release the heat as the latent heat when they are in the
198 melting and solidifying temperature range (usually $\pm 3^{\circ}\text{C}$ from the melting and solidification
199 point) and as the sensible heat during the rest of time [27]. Thus, the composite energy storage
200 materials helped to maintain the water temperature higher even during the late evening and
201 nocturnal hours to get maximum productivity.

202

203 **4. Results and Discussion**

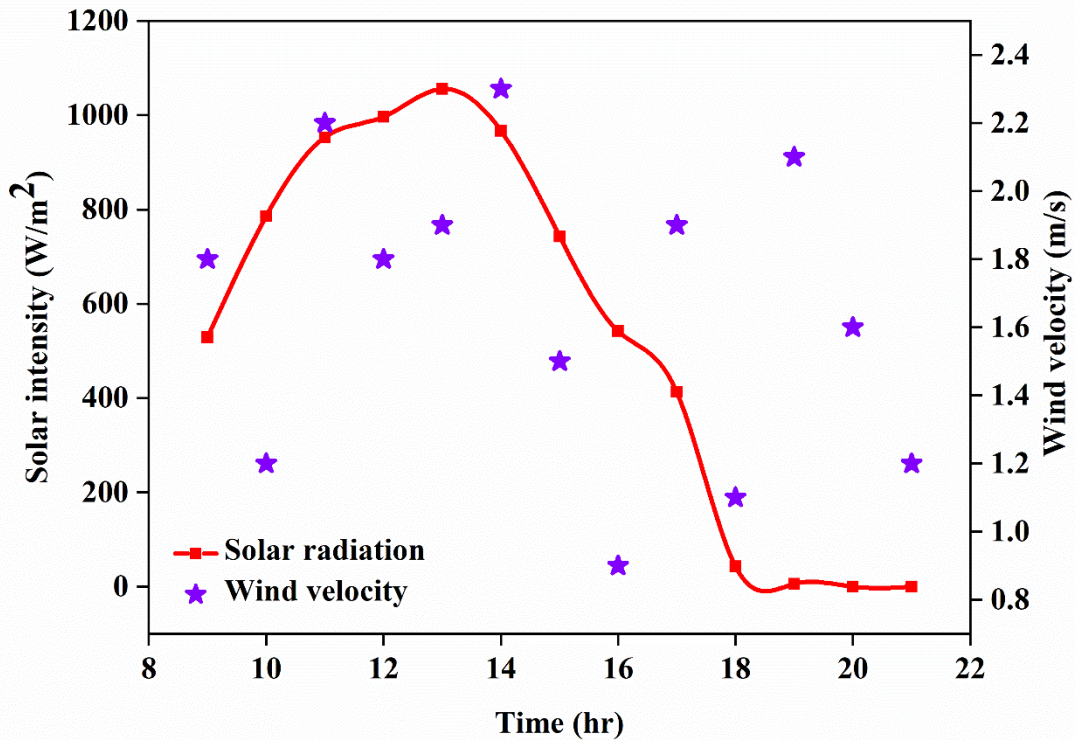
204 The results related to the investigations (i.e. technical, economic, enviro-economic, energy
205 matrices analysis and water quality test) carried out in this study are discussed under the
206 following sections.

207 **4.1. Technical investigations**

208 The effects of climatic parameters during experimentation and temperature of the various
209 components (glass, water, energy storage materials) associated with the conventional and
210 modified still are discussed in the following sub-sections. Furthermore, the melting and
211 solidification characteristics of the phase change material along with the hourly and daily yield
212 of the conventional and modified still are discussed in detail. Also, to aid comparison, the
213 productivity of the present study is compared against the existing literature at the end of this
214 section.

215 4.1.1. Effect of climatic parameters

216 The hourly variation of the solar intensity and wind velocity is depicted in Fig. 5. It was
217 observed that the intensity gradually increased from 9:00 h and reached its maximum intensity
218 (1056 W/m^2) at 13:00 h and then seamlessly dips down to zero during the late evening hours.
219 The peak intensities were observed during 13:00 h, 12:00 h, and 14:00 h corresponding to 1056
220 W/m^2 , 997 W/m^2 and 967 W/m^2 , respectively. A parabolic trend was observed in the intensity
221 profile of the solar radiation during the entire span of the experiment.



222

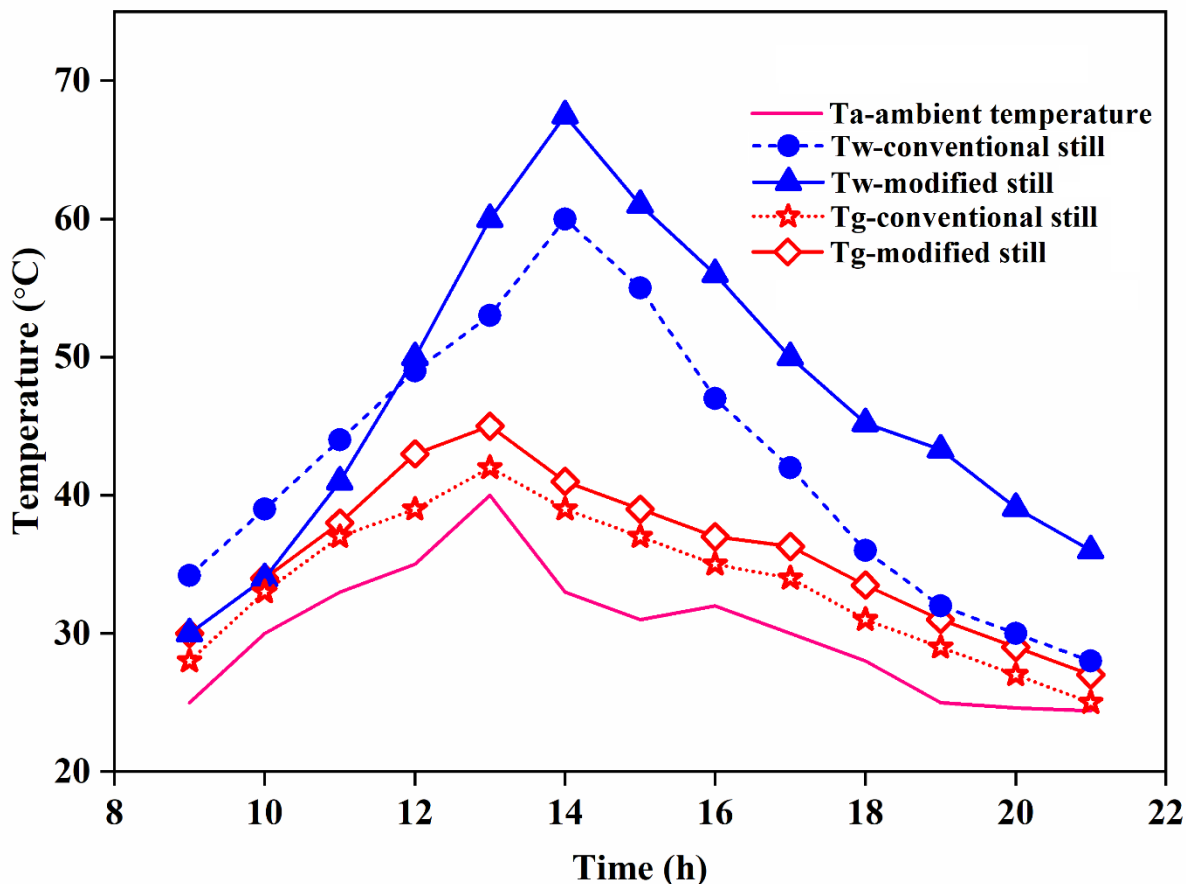
223 **Fig. 5. Hourly variations of solar intensity and wind velocity during the experiment**

224 The maximum, minimum and average wind velocity observed was 2.4 m/s , 0.9 m/s and 1.6
225 m/s , respectively. These velocities are sufficiently small not to affect the experimental
226 observations [17,84].

227 4.1.2. Effects of the glass and water temperatures

228 The glass and water temperatures of the modified still were greater than the corresponding
229 temperatures of the conventional still after 12:00 h (Fig. 6). This increase was due to the
230 addition of ferrite magnets, graphite plates and phase change material (PCM) in the modified
231 still. The better thermal conductivity of sensible heat energy storage material (which was in
232 direct contact with water) along with the presence of PCM have considerably decreased the
233 water temperature in the modified still during the initial stage of the experiment (i.e. till 12:00
234 h) as compared to the conventional still. During 9:00-12:00 h, the heat energy from the water

235 was absorbed by the graphite plates, ferrite magnets and phase change material (i.e. during
 236 charging of PCM). After 12:00 h, the absorbed heat was gradually released to the water which
 237 in turn further increased the temperature of the water (discharging of PCM) [27,85]. Also, this
 238 mechanism helped the water to maintain its temperature at a higher level even during nocturnal
 239 hours.
 240

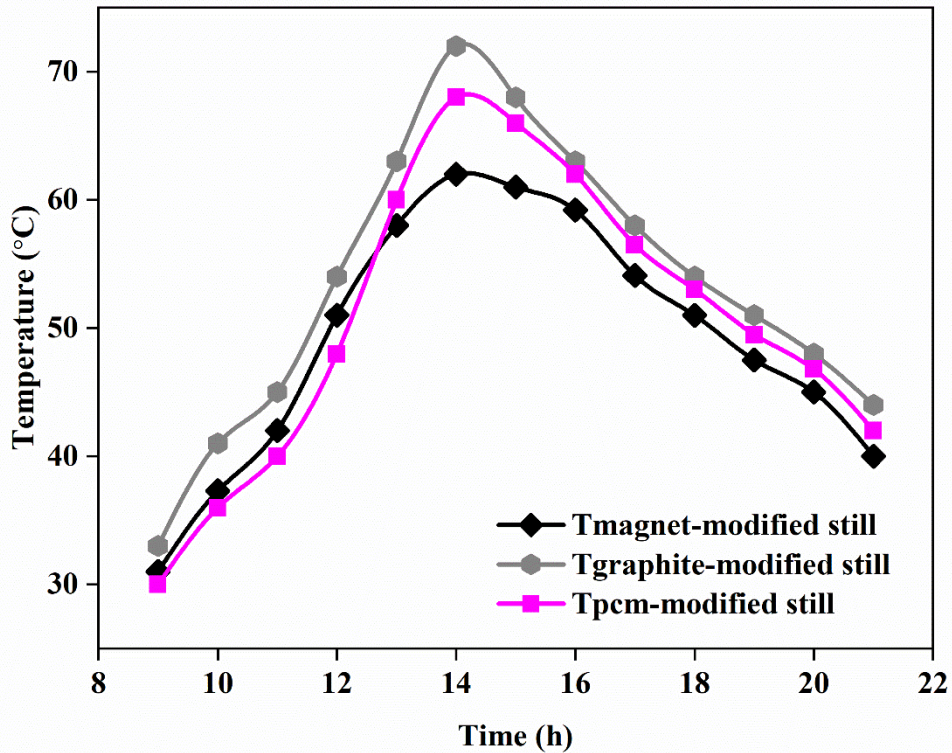


241
 242 **Fig. 6. Hourly variations of glass, water and ambient temperatures for conventional and**
 243 **modified still**

244 A peak trend was observed from 15:00 h to 19:00 h showing the maximum variation in the
 245 water temperature of the modified still as compared to the conventional still. During this time,
 246 PCM was in the range of its peak solidification temperature wherein it released its latent heat
 247 completely [27,85]. In addition to this, the graphite plates also released its heat to the water,
 248 which accounted for a substantial increase in the water temperature. Due to these reasons, the
 249 water temperature was significantly higher for the modified still than the conventional still. In
 250 summary, the integration of composite thermal energy storage along with ferrite magnets have
 251 augmented the water temperature of the modified still.

252 4.1.3. Effects of integrated energy storage materials

253 The temperature variations of the various storage materials in the modified still are
254 presented in Fig. 7. The temperature of the phase change material was considerably low as
255 compared to the magnet temperature during the first four hours of the experiment. This was
256 because the melting characteristics (melting time) of the PCM was higher as compared to the
257 magnet. Moreover, the magnet was in direct contact with the water which enabled the magnet
258 to increase its temperature till 12:00 h.



259
260 **Fig. 7. Temperature variations of composite thermal energy storage materials and ferrite**
261 **magnets in the modified still.**

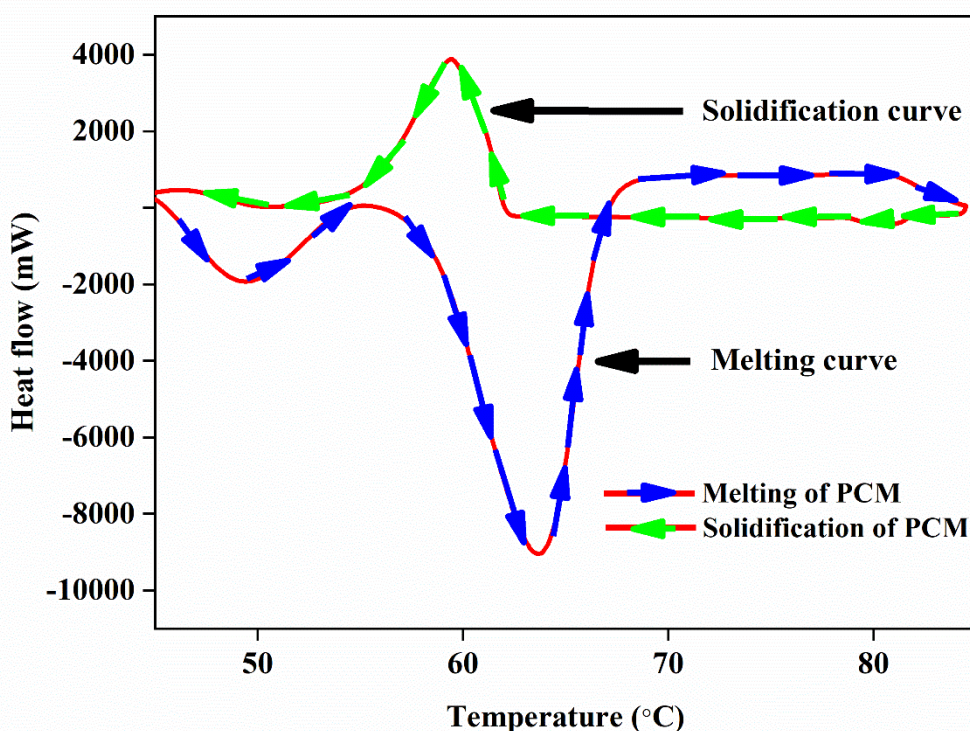
262 Furthermore, it also acted as an additional heat source allowing the water to maintain a
263 higher temperature during the cloudy hours. The maximum temperature of magnet, graphite
264 and PCM was observed to be 62°C, 72°C and 68°C, respectively at 14:00 h. A 16% and 6%
265 increase in the temperature was accounted for graphite plate comparing the magnet and PCM
266 temperatures (at 14:00 h), respectively. During the late evening hours (17:00 h to 21:00 h),
267 graphite plate and PCM temperatures dominated the temperature of the magnet. There was a
268 2-4% increase in the temperatures of the PCM and graphite plate as compared to the magnet's
269 temperature.

270 The graphite plates consistently extend their supremacy over the other two materials
271 throughout the experiment due to the high thermal conductivity. In summary, the melting and

272 solidification characteristic of PCM (which is discussed below) moderated the temperature
273 variation across the storage unit beneath the basin. Furthermore, the energy storage units
274 temperature played a vital role in governing the water temperature to increase the temperature
275 difference with that of glass temperature and in turn, increased the productivity.

276 4.1.4. Effects of melting and solidification characteristics of PCM

277 The melting and solidification characteristics of the latent heat energy storage material (i.e.
278 paraffin) are depicted in Fig. 8. The melting commenced at 52°C and gradually reached its peak
279 melting temperature of 64°C. There was a 20% difference in the temperature between the start
280 and peak melting temperature of the paraffin. Thus, there was considerable latent heat absorbed
281 by paraffin between 52°C and 64°C. The peak melting and solidification temperatures of the
282 paraffin were found to be 64°C and 58°C, respectively.



283

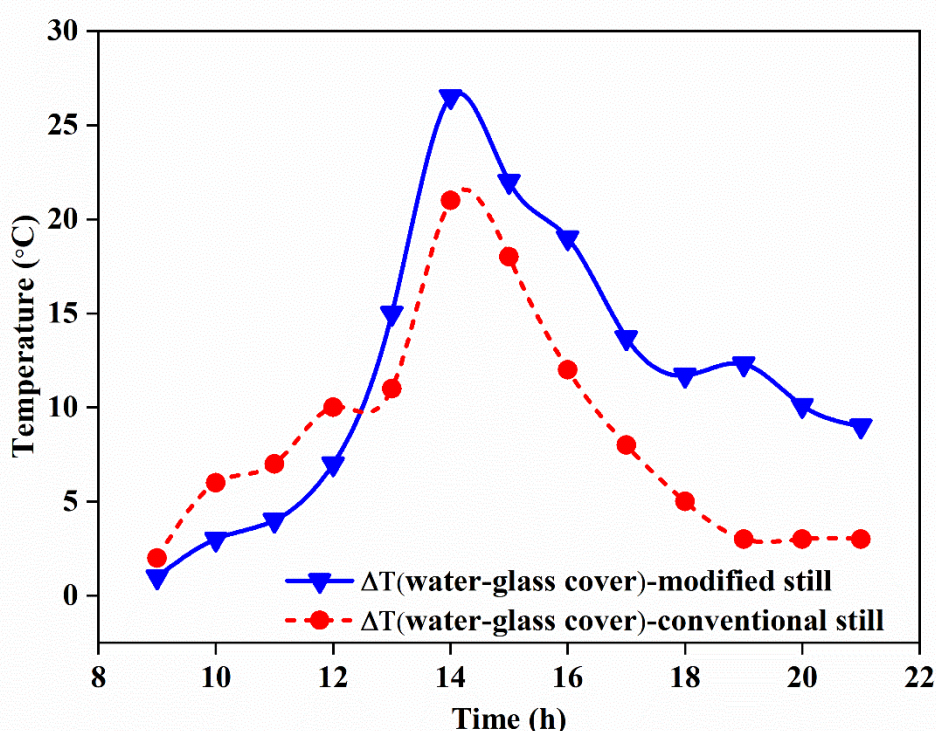
284 **Fig. 8. Melting and solidification characteristics of PCM**

285 The solidification starts at 61°C and lasts till 53.5°C contributing a 7.5°C temperature
286 difference with a 14.5% increase in the amount of latent heat released during solidification.
287 The PCM has released its latent heat till 53.5°C during solidification, inducing a greater
288 temperature difference between water and glass cover increasing the daily yield. Thus, the
289 addition of latent heat energy storage material has acted as an additional heat source to increase
290 the water temperature in the modified still as compared to the conventional still. The prolonged
291 melting and solidification behavior of the paraffin made a significant contribution in melting

292 and solidifying characteristics by absorbing and releasing considerably a higher amount of the
293 latent heat during the charging and discharging process, respectively.

294 4.1.5. Effect of the temperature difference between water and glass cover

295 The temperature difference plays an important role in augmenting the hourly and
296 cumulative yield of the solar still [27,35,42]. Fig. 9 depicts the difference in temperatures of
297 water and glass cover for conventional and modified still. The maximum temperature
298 difference of 26.5°C (at 14:00 h) was observed in the modified still whereas the maximum
299 temperature difference observed in the conventional still was only 21°C (at 14:00 h). A 26%
300 increase was observed in the peak temperature differences between the water and glass cover.



301
302 **Fig. 9. Comparison of the temperature difference between water and glass cover for the**
303 **conventional and modified still**

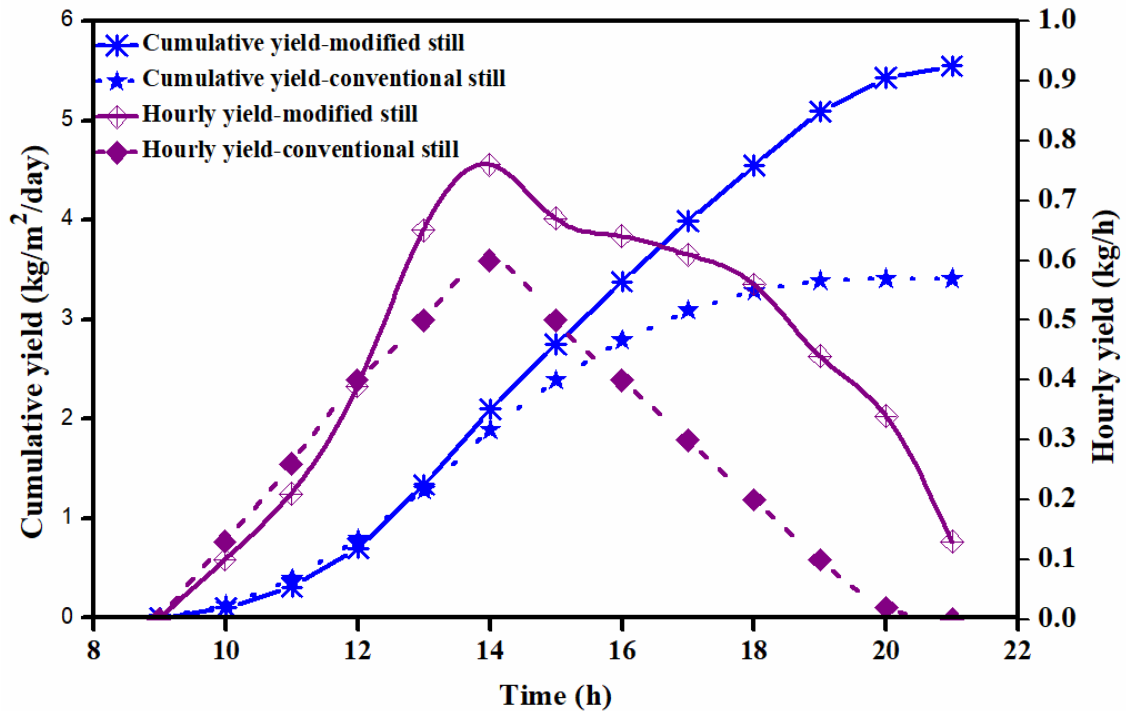
304 At 9:00 h, 10:00 h, 11:00 h and 12:00 h, the temperature difference between water and glass
305 cover was higher in the modified still as compared to the conventional still. There was a 4°C
306 increase observed in the temperature difference of water and glass cover for the modified still
307 over the conventional still from 9:00 h to 12:00 h. The main reason behind this variation was,
308 the energy storage materials were charged during 9:00 h to 12:00 h, where the heat energy of
309 the water was absorbed by the sensible and latent heat energy storage materials which in turn
310 decreased the water temperature in the modified still as compared to the conventional still.

311 After 12:00 h, there was an increasing trend observed in the temperature difference between
312 the water and glass cover of the modified still. This was because, after 12:00 h, the energy
313 storage materials have released the heat back to the water, thus increasing the temperature of
314 the water in the modified still to be more than that of the conventional still (see Fig. 7) [27,85].
315 Also, it was the same reason for achieving a higher temperature difference (9°C) even during
316 late evening hours in the modified still. In summary, the temperature difference between water
317 and glass cover was higher for the modified still after 12:00 h due to the integration of paraffin,
318 ferrite magnets and graphite plates – which helped the modified still to achieve better
319 productivity over the conventional still.

320 *4.1.6. Variation of hourly yield and daily productivity*

321 The hourly and daily productivity comparison of the conventional and modified still is
322 depicted in Fig. 10. The hourly yield of the conventional still was slightly higher than the
323 modified still till 12:00 h. After 12:00 h, the hourly yield of the modified still exceeds the
324 conventional still. The maximum hourly yield obtained for conventional and modified still was
325 0.6 and 0.7 kg/m²/day, respectively contributing to a 26.6% enhancement in the modified still
326 over the conventional still.

327 The results show that even in the late evening hours (i.e. from 17:00 h to 21:00 h), there
328 was a constant hourly output achieved in the modified still. The evening time productivity of
329 the conventional and modified still ranged from 0.3 kg/h to 0.02 kg/h and 0.6 kg/h to 0.1 kg/h,
330 respectively. The daily average cumulative yield for the conventional and modified still was
331 found to be 2 kg/m²/day and 2.7 kg/m²/day, respectively. The percentage increase in the
332 average cumulative yield of the modified still accounted for 33% as compared to the
333 conventional still. The cumulative yield of conventional and modified still was 3.4 kg/m²/day
334 and 5.5 kg/m²/day, respectively. There was a 62% increase in the daily cumulative yield of the
335 modified still as compared to the conventional setup. Evening time productivity (i.e. from
336 17:00 h to 21:00 h) for the conventional still was accounted for less than one liter whereas it
337 was doubled (nearly 2 liters) for the modified still. There was a 235% increase in the yield
338 observed during evening time in the modified still as compared to the conventional still. This
339 variation was due to the fact that the magnetic field has a positive impact on the evaporation
340 rate due to the change in hydration shells of the water in the modified still [86]. The magnetic
341 field has increased the rate of evaporation, due to which the productivity enhancement was
342 increased to 62%, compared to only 50.3% enhancement in studies using graphite and PCM
343 but without any magnets [24]. This clearly indicates that a 12% increment in the enhancement
344 was due to the magnetic field.



345
346 **Fig. 10. Variation of hourly and cumulative yield for the conventional and modified still**

347 Effective separation of salt from the water was possible when the solutions were
348 circulated in a magnetic field. The variation in the hourly and cumulative yield was due to the
349 addition of magnets which reduced the surface tension and increased the evaporation rate of
350 the water. And, the integration of composite energy storage materials with the still acted as an
351 additional heat source and helped to maintain the water temperature higher even during late
352 evening and nocturnal hours. Thus, the variation in the hourly yield was because of the
353 combined effect of composite energy storage and magnetizing effect by the thermal energy
354 storage materials (paraffin and graphite plates) and ferrite magnets, respectively.

355 *4.1.7. Productivity comparison of the present study with existing literature*

356 A detailed comparison of the daily yield of the present study with the existing literature is
357 summarized in Table 6. Shalaby et al. (2016) [67] used paraffin as the latent heat storage
358 material under Egyptian climatic conditions and achieved productivity of 3.7 kg/m²/day which
359 was 46.2% lesser than the productivity of the present study. In the same year, Mousa and
360 Gujrathi (2016) [62] also have performed their study using paraffin as the latent heat storage
361 material in Oman and obtained a daily yield of 2.1 kg/m²/day which was 61.8% lesser than the
362 productivity achieved by the current study. Rufuss et al. (2018) [27] performed experiments
363 using nanoparticles i.e. titanium dioxide and copper oxide enhanced paraffin under Indian
364 climatic conditions and achieved a daily yield of 4.9 kg/m²/day and 5.2 kg/m²/day, respectively

365 which are 4% and 11.3% lesser than the productivity of the present study. Kabeel et al. (2019)
 366 [68] have experimented with both latent and sensible heat energy storage materials i.e. by using
 367 paraffin and black gravel, respectively under Egyptian climatic conditions and reported a daily
 368 yield of 3.2 kg/m²/day which was 40.5% lesser than the present study's productivity. Diwakar
 369 et al. (2020) [56] and Sharshir et al. (2020) [87] have, respectively used gravel coarse aggregate
 370 and linen wicks with carbon black nanoparticles as sensible heat storage materials and achieved
 371 a daily cumulative yield of 4.2 kg/m²/day and 5.2 kg/m²/day, respectively corresponding to
 372 31% and 4.3% less yield than the current study.

373 To summarise, the productivity of the current study (5.5 kg/m²/day) is greater than previous
 374 results, due to the combined effect of magnets and composite energy storage materials.

375 **Table 6. Productivity comparison of the present study with the existing literature (where data**
 376 **are provided)**

Sl. No	Authors and references	Type of energy storage techniques	Type of Energy storage material	Location	Productivity (kg/m²/day)
1	Shalaby et al. (2016) [67]	Latent heat energy storage	Paraffin	Egypt	3.76
2	Mousa and Gujarathi., 2016 [62]	Latent heat energy storage	Paraffin	Oman	2.1
3	Rufuss et al., [27]	Latent heat energy storage	Paraffin and CuO nanoparticle	India	5.28
4	Diwakar et al. (2020) [56]	Sensible heat energy storage	Gravel coarse aggregate	India	4.21
5	Rufuss et al., 2018 [27]	Latent heat energy storage	Paraffin enhanced with TiO ₂ nanoparticles	India	4.94

6	A.E. Kabeel et al. 2019 [68]	Latent heat and sensible heat energy storage	Paraffin and Black gravel	Egypt	3.27
7	Sharshir et al., 2020 [87]	Sensible heat energy storage	linen wicks and carbon black nanoparticles	Egypt	5.26
8	Present study	Latent heat and sensible heat energy storage	Paraffin, Ferrite Magnets, Graphite plates	India	5.5

377

378 4.2.Economic investigations

379 The economic parameters such as capital cost, annual cost, salvage value, annual
380 maintenance cost and cost per liter for the conventional and modified still were discussed in
381 the following section. A detailed cost per liter comparison of the present study with the existing
382 literature was also presented at the end of this section

383 4.2.1. Economic analysis

384 Various costs and economic parameters such as fixed annual cost (FAC), annual
385 maintenance and operational cost (AMC), annual productivity (M), productivity percentage
386 and cost per liter (CPL) associated with the experiments were calculated using the following
387 formulae (Eqs. 1-9) suggested in the literature [27,88]

$$388 \quad \text{FAC} = P \times \text{CRF} \quad (1)$$

$$389 \quad \text{SFF} = \frac{i}{(i + 1)^{y-1}} \quad (2)$$

$$390 \quad S = 0.2 \times P \quad (3)$$

$$391 \quad \text{ASV} = \text{SFF} \times S \quad (4)$$

$$392 \quad \text{AMC} = 0.15 \times \text{FAC} \quad (5)$$

$$393 \quad \text{AC} = \text{FAC} + \text{AMC} - \text{ASV} \quad (6)$$

394 where P, CRF, SFF, S, AC are the present capital cost, capital recovery factor, sinking fund
395 factor, salvage value and annual cost, respectively. The capital recovery factor (CRF) and total
396 years of operation (y) are assumed to be 0.17 and 10 years, respectively [27]. The average
397 productivity (M) was calculated by

$$398 \quad M = c \times n \quad (7)$$

399 where ‘c’ is the distillate yield per day and ‘n’ is considered to be approximately 250 days. The
 400 productivity percentage can be calculated using the ratio of the product of annual productivity
 401 and selling price of water (\$0.2/l) to the annual cost [27]. Then, the cost per liter (CPL) of
 402 distilled water can be calculated by the ratio of annual cost and average annual productivity

$$403 \quad \text{Productivity (\%)} = \frac{\text{Annual productivity} \times \text{selling price of the water}}{\text{annual cost}} \quad (8)$$

$$404 \quad \text{CPL} = \frac{\text{AC}}{\text{M}} \quad (9)$$

405 The total cost acquired for the conventional and modified still was \$82 and \$126,
 406 respectively which includes the cost of the basin, stand, insulation, adhesives, glass cover,
 407 magnets (for modified still only), graphite plate (for modified still only), paraffin (for modified
 408 still only), paints and fabrication costs (see details in Table 7). The total cost of the modified
 409 still was 55% greater than the conventional still, due to the integration of ferrite magnets,
 410 graphite plates and paraffin which contribute to 4.7%, 24% and 6.3%, respectively in the total
 411 cost of the modified still. The largest cost component (up to 24%) corresponded to the graphite
 412 plates, because of the manufacturing complexity associated with the graphite material. Thus, it
 413 is summarized that even though there was a 55% increase in the total cost of the modified still
 414 as compared to the conventional still, the other economic parameters like cost per liter and
 415 annual productivity are duly important for arriving at a decision about the economic feasibility
 416 of the entire experiment.

417 The various costs associated with the conventional and modified still are shown in Table
 418 8. The fixed annual cost (FAC) and salvage value were \$22.2 and \$25, respectively which
 419 contributed to a 54% increase in the value comparing the conventional still. The increase in
 420 FAC and salvage of the modified still was due to the direct accounting of present capital cost
 421 in calculating the FAC (see Eq. 1).

422 Furthermore, the present capital cost was directly proportional to the FAC and salvage
 423 value. The AMC of the modified still was 55.3% higher than the conventional still because of
 424 the integration of graphite plates and ferrite magnets. This also includes the additional
 425 maintenance area/operation cost on the inclusion of PCM materials (paraffin) underneath the
 426 basin. The average annual productivity of the modified still was significantly higher (62%) as
 427 compared to the conventional still due to the higher distillate yield per day in the modified still
 428 (5.5 kg/m²/day) which confirms its advantage in terms of yearly performance. There was a 33%
 429 increase in the productivity percentage of the modified still in comparison with the
 430 conventional still contributing to 840% and 807%, respectively.

Table 7. Capital cost of the experiment (conversion rate of INR 74.76 per US\$ was used)

Components	Conventional still (US\$)	Modified still (US\$)
Basin	25	25
Insulation	7	7
Stand	12	12
Transparent cover	8	8
Graphite plates	0	30
Ferrite magnets	0	6
Aluminium paint	3.31	3.31
Adhesive gum	2.65	2.65
Foam strap	4	4
Paraffin wax	0	8
Fabrication cost	20	20
Total cost	82	126

432

433 Table 8 shows that the CPL of conventional and modified still was \$0.018 and \$0.017,
 434 respectively. The CPL of the modified still was 3.7% lower than the CPL of the conventional
 435 still. Even though the total cost of modified still (See Table 7) was 55% higher than the
 436 conventional still, the CPL was 3.7% lesser for the modified still as against the conventional
 437 still. This variation was due to the combined accounting of annual cost, maintenance cost and
 438 average annual productivity in arriving at the CPL. Thus, the modified still gives economically
 439 cheaper water as compared to the conventional still. The comparison of CPL of the present
 440 study with the existing literature is certainly important to quantify the obtained result and hence
 441 the following section compares the CPL of the current study with the literature.

442 **Table 8. Cost analysis of modified still with integrated sensible and latent heat energy storage in**
 443 **comparison with conventional still**

Parameters in US\$	Conventional still	Modified still
Present capital cost (P)	81	125.9
Capital Recovery Factor(CRF)	0.17	0.17
Fixed Annual Cost (FAC)	14.3	22.2
Salvage value(S)	16.2	25.1

Sinking Fund Factor (SFF)	0.04	0.04
Annual Salvage Value (ASV)	0.7	1
Annual Maintenance Operational Cost (AMC)	2.1	3.3
AC (Annual Cost)	15.7	24.5
M (Average Annual Productivity) in liters	850	1375
Productivity (%)	807.6	840.5
CPL (Cost of distilled water Per Liter)	0.018	0.017

444

445 *4.2.2. Cost per liter comparison of the present study with existing literature*

446 Table 9 compares the cost per liter (CPL) of the present study with the existing literature.
447 The CPL of the present study was \$0.017 which was found to be 78%, 81%, 40%, 37%, 32%,
448 87%, 71%, 6%, and 0.8%, respectively cheaper than the CPL of freshwater from the solar still
449 with paraffin [67], wick [67], paraffin [60], titanium dioxide nanoparticles enhanced paraffin
450 [27], copper oxide nanoparticles enhanced paraffin [27], graphene oxide enhanced paraffin
451 [27], gravel coarse aggregate [56], paraffin with black gravel [68] and linen wicks with carbon
452 black nanoparticles [87]. This huge range of the percentage difference (min: 0.3% and max:
453 78%) in the CPL of the present study with other studies may be due to the capital cost of the
454 studies, which includes fabrication cost, availability and price of the materials required for
455 fabrication (basin material, insulation and stand) in the respective location during the year of
456 experimentation. Also, the difference may be due to the rate of interest and years of operation
457 assumed for the economic analysis.

458 Thus, it is concluded from the above assessment that the CPL of the modified still is
459 considerably cheaper. The main reason is the combined stimulus of the improved daily yield
460 and an annual yield of the modified still due to the integration of magnets, graphite plates and
461 PCM materials.

462 **Table 9. Comparison of CPL of the present study with the existing literature (where data are**
463 **provided)**

Sl. No	Authors and references	Type of energy storage technique	Type of energy storage material	Country	CPL (\$)
1.	Shalaby et al., 2016 [67]	Latent heat	Paraffin	Egypt	0.08
2.	Shalaby et al., 2016 [67]	Latent heat and sensible heat	Paraffin and wick	Egypt	0.09

3.	Kabeel and Abdelgaied., 2016 [60]	Latent heat	Paraffin	Egypt	0.03
4.	Rufuss et al., 2018 [27]	Latent heat	Paraffin	India	0.03
5.	Rufuss et al., 2018 [27]	Latent heat	Paraffin enhanced with TiO ₂ nanoparticles	India	0.028
6.	Rufuss et al., 2018 [27]	Latent heat	Paraffin enhanced with CuO nanoparticles	India	0.026
7.	Rufuss et al., 2018 [27]	Latent heat	Paraffin enhanced with GO nanoparticles	India	0.13
8.	Diwakar et al. 2020 [56]	Sensible heat	Gravel coarse aggregate	India	0.06
9.	Kabeel et al., 2019 [68]	Latent heat and sensible heat	Paraffin and Black gravel	Egypt	0.01
10.	Sharshir et al., 2020 [87]	Sensible heat	linen wicks and carbon black nanoparticles	Egypt	0.01
11.	Present study	Latent heat and sensible heat	Paraffin, Ferrite Magnets, Graphite plates	India	0.017

464

465 *4.2.3. Comparison of the CPL from the present study with the cost of bottled water in*
466 *India*

467 Generally, the cost of bottled water and the selling price of bottled water in India are \$0.06
468 per liter and \$0.22 per liter, respectively [27,89]. These values are 69% and 91.6% higher than
469 the CPL of the freshwater obtained from the modified still studied here. Thus, the CPL from
470 the modified still was 69% and 91.6%, respectively cheaper than the bottled water cost and
471 typical selling price of bottled water in India.

472 **4.3. Enviro-economic investigation**

473 The enviro-economic analysis estimates the amount of carbon dioxide, oxides of sulphur
474 and nitrogen emitted for a lifetime from the modified still (Eqs. 10-15). Furthermore, it gives
475 the details about the total embodied energy of the system along with the details of the total

476 carbon dioxide mitigated and the corresponding carbon credit earned. These parameters can be
 477 calculated by the following formulae suggested in the literature [90–93]. Various
 478 environmental parameters like total embodied energy, emissions (CO₂, SO₂, and NO), the total
 479 amount of CO₂ mitigated and the carbon credit earned from the modified still are discussed
 480 under the following section:

481 The total amount of CO₂ emitted for a lifetime is calculated using the following formula

$$482 \quad \text{CO}_2 \text{ emitted for a lifetime} = \text{Embodied energy} \times 1.58 \quad (10)$$

483 Similarly,

$$484 \quad \text{SO}_2 \text{ emitted for a lifetime} = \text{Embodied energy} \times 0.012 \quad (11)$$

$$485 \quad \text{NO emitted for a lifetime} = \text{Embodied energy} \times 0.005 \quad (12)$$

486 The net carbon dioxide mitigated for the lifetime can be calculated using

$$487 \quad \text{Net CO}_2 \text{ mitigation for lifetime} \\ 488 \quad = [(\text{Embodied energy (out)} \times n) - \text{Embodied energy}] \quad (13)$$

489 where 'n' is the total number of years. The embodied energy of the system and the carbon
 490 credit earned by the system is calculated by

$$491 \quad \text{Embodied energy (out)} = \frac{\text{Annual yield} \times \text{latent heat}}{3600} \quad (14)$$

$$492 \quad \text{Carbon credit earned} = \text{Net CO}_2 \text{ mitigation for lifetime} \times 9.99 \quad (15)$$

493 4.3.1. Total embodied energy

494 The embodied energy along with the concomitant energy density and mass of various
 495 materials used in the modified solar still [56,69,90–96] are tabulated in Table 10. The
 496 estimation of total embodied energy is necessary to estimate the CO₂, SO₂ and NO emissions
 497 and other enviro-economic parameters. The glass had a total mass of 1.1 kg with the highest
 498 energy density of 1127 kWh/kg as compared to the other associated components and it carried
 499 the embodied energy of 45 kWh. Mild steel stand, frame and clamp had the maximum
 500 embodied energy of 180.5 kWh due to the heavier mass (19 kg) and energy density (of 9.5
 501 kWh/kg) of the individual structures. Both the basin and latent heat energy vessel beneath the
 502 basin were made up of aluminium with an equivalent mass, energy densities and embodied
 503 energy of 4 kg, 13.5 kWh/kg and 54.2 kWh, respectively. The basin liner had a mass of 0.2 kg
 504 with an energy density of 25.1 kWh/kg contributing to 1.6% of the total embodied energy (6.2
 505 kWh/kg). The other components such as insulation gasket and insulators had a total energy
 506 density of 8.8 kWh/kg and occupied 2.2% of the total embodied energy. The enhancement
 507 techniques additionally used in the modified solar still are graphite plates, ferrite magnets and
 508 paraffin wax which contribute embodied energy of 25.4 kWh, 18.3 kWh and 0.48 kWh,
 509 respectively. Thus, arriving at the total embodied energy for the whole modified system (of

510 393.3 kWh) by the summation of the embodied energy of all the individual system components.
 511 The estimated embodied energy from this analysis will be taken as an input for estimating the
 512 various enviro-economic parameters in the rest of the enviro-economic analysis.

513 **Table 10. The total embodied energy of the modified still [56,69,90–96]**

Components	Mass (kg)	Energy	
		density (kWh/kg)	Embodied energy (kWh)
Glass	1.1	11127	45
MS stand + Frame + Clamp	19	9.5	180.5
Basin (Aluminium)	4	13.5	54.2
Basin liner	0.2	25.1	6.2
Insulation gasket	1.8	3.3	5.9
Insulator	1.5	1.9	2.8
Graphite Plate (14 Nos)	2.8	9.0	25.4
Ferrite Magnets (10 Nos)	2	9.1	18.3
Latent heat energy storage material holder beneath the basin (Aluminium)	4	13.5	54.2
Paraffin wax	10	0.04	0.4
Total Embodied energy			393.3

514

515 *4.3.2. Carbon dioxide emission, mitigation and carbon credit earned*

516 Table 11 presents various details about the emissions (CO₂, SO₂, and NO), CO₂ mitigation,
 517 carbon credit, energy payback time and life cycle conversion efficiency of the modified still.
 518 The amount of CO₂, SO₂, and NO emitted for a lifetime from the modified still were found to
 519 be 621.4 Tonnes, 4.7 Tonnes and 1.9 Tonnes, respectively. The energy payback time will be
 520 lesser for the systems with low embodied energy since the embodied energy is directly
 521 proportional to the energy payback time and the net CO₂ mitigation. In summary, it is advisable
 522 to use materials with less embodied energy value to reduce emissions like CO₂, SO₂, and NO
 523 and minimise the energy payback time.

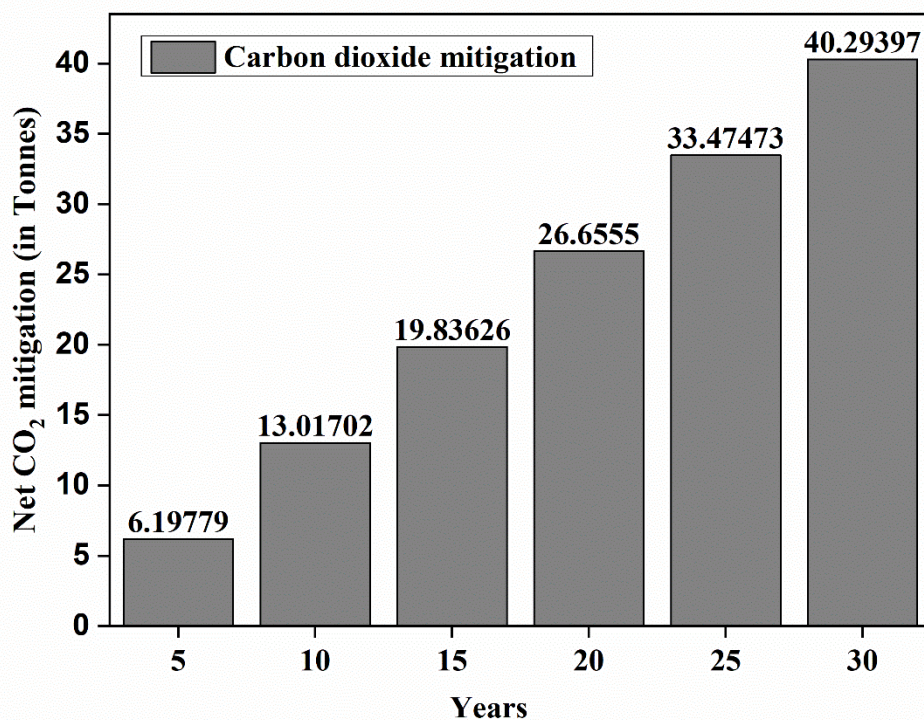
524 **Table 11. Carbon dioxide emission, CO₂ Mitigation, Carbon credit earned and energy matrices**
 525 **for the modified still**

Sl. No	Parameters	Values
1	Embodied energy	393.3
2	Emission of CO ₂ for lifetime	621.4

3	Emission of SO ₂ for lifetime	4.7
4	Emission of NO for lifetime	1.9
5	Net carbon dioxide mitigation during 10 th year (in Tonnes)	13
6	Carbon credit earned during 10 th year (in US\$)	130
7	Net carbon dioxide mitigation during 15 th year (in Tonnes)	19.8
8	Carbon credit earned during 15 th year (USD)	198
9	Energy payback time (Years)	0.4
10	Energy production factor	2.1
11	Life cycle conversion efficiency	0.2

526 *4.3.3. Carbon dioxide Mitigation*

527 The net CO₂ mitigated from the modified still is presented in Fig. 11. Carbon dioxide
528 mitigated increased from 6.2 Tonnes to 40.2 Tonnes over the years (i.e. from 5 years to 30
529 years), respectively. Also, there was a constant increase of 7 Tonnes in the net CO₂ mitigated
530 in the current year over the preceding year.



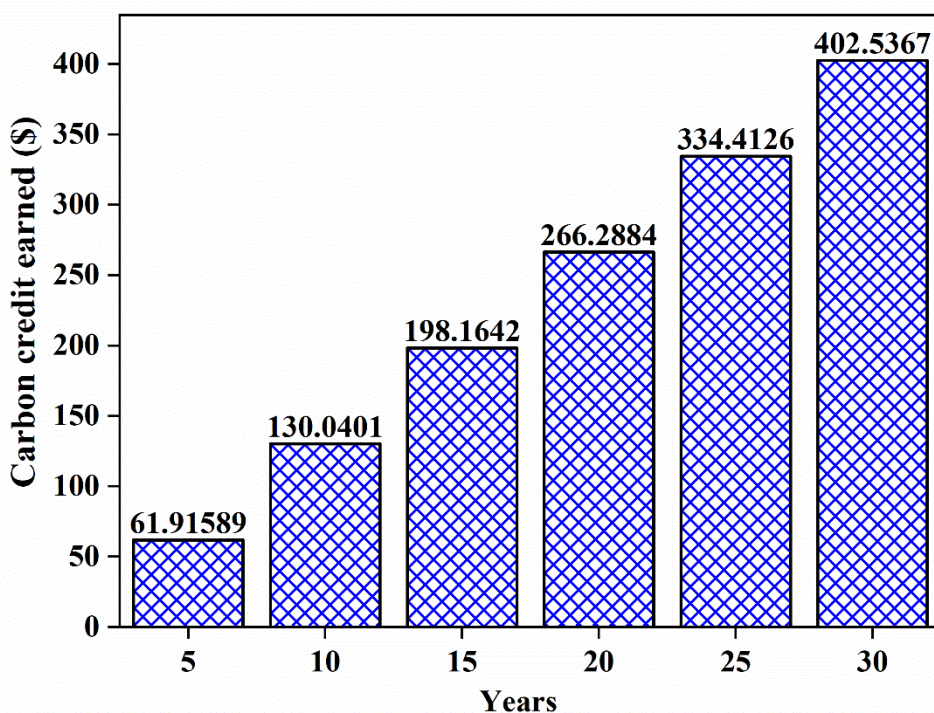
531

532 **Fig. 11. Yearly variation of the net carbon dioxide mitigated from the modified still**

533 There was a 110% increase in the net carbon dioxide mitigated for the first five years (6.2
 534 Tonnes) as compared to net CO₂ mitigated for the tenth year (13 Tonnes). This percentage
 535 further reduced to 52.4%, 34.3%, 25.5% and 20.3% at the end of the 15th, 20th, 25th, and 30th
 536 years, respectively corresponding to a net CO₂ mitigated value of 19.8 Tonnes, 26.6 Tonnes,
 537 33.4 Tonnes and 40.2 Tonnes. Ideally, for a solar desalination system, the average total number
 538 of years can be considered as 15 years [91] and citing that, at the end of the 15th year, the total
 539 CO₂ mitigated from the modified still of the present study will be 19.8 Tonnes.

540 *4.3.4. Carbon credit earned*

541 The overall carbon credit earned for the modified still in the present study is shown in Fig.
 542 12. The carbon credit is the net amount of CO₂ mitigated which can be sold for monetary value.
 543 The carbon credit earned for the mitigation of 6.2 Tonnes (during 5th year), 13 Tonnes (during
 544 10th year), 19.8 Tonnes (during 15th year), 26.6 Tonnes (during 20th year), 33.4 Tonnes (during
 545 25th year) and 40.2 Tonnes (during 30th year) of carbon dioxide was \$61, \$130, \$198, \$266,
 546 \$324 and \$402, respectively.



547 **Fig. 12. Yearly variation of the carbon credit earned for the modified still**

549 Thus, the modified still with paraffin, graphite plates and ferrite magnets used in the present
 550 study earns \$66 (on average) more than the credit earned in the present year in comparison
 551 with the credit earned after the preceding five years.

4.4. Energy matrices analysis

This section includes a discussion about the energy payback time, energy production factor and life cycle conversion efficiency. The various components of energy matrices include energy production factor, energy payback time and life cycle conversion efficiency (Eqs. 16–18). The energy matrices are calculated using the formulae suggested in the studies [56,90–93]. The energy payback time is the period that takes to repay the amount of energy used by the setup. The energy production factor is the inverse of energy payback time.

$$\text{Energy payback time} = \frac{\text{Embodied energy}}{\text{Amount of energy production per year}} \quad (16)$$

Energy production factor is calculated by the formula given below

$$\text{Energy production factor} = \frac{\text{Amount of Energy produced per year}}{\text{Embodied Energy}} \quad (17)$$

The life cycle conversion efficiency can be calculated by

$$\begin{aligned} &\text{Life cycle conversion efficiency} \\ &= \frac{\text{Net carbon dioxide mitigated for lifetime}}{\text{Annual solar energy} \times \text{life span of the system}} \end{aligned} \quad (18)$$

Parameters like energy production factor, energy payback time and life cycle conversion efficiency are used in energy matrices. A system with higher embodied energy will consume more energy and in turn emits a higher amount of CO₂ to the atmosphere which results in increasing the energy payback time [56,90]. The energy payback time and energy production factor for the modified system were found to be 0.4 years (5.4 months or 164 days) and 2.1, respectively (Table 12). The year-wise life cycle conversion efficiency of the modified solar still is shown in Fig. 13.

The maximum life cycle efficiency achieved for the proposed modified still was 0.52 at the end of the 30th year. The life cycle conversion efficiency of the modified still during the 10th, 15th, 20th, 25th, and 30th year was found to be 0.17, 0.26, 0.34, 0.43 and 0.52, respectively contributing to an increase of 52%, 30%, 29% and 20% in the life cycle conversion efficiency of the modified still for each year, respectively over the preceding five years.

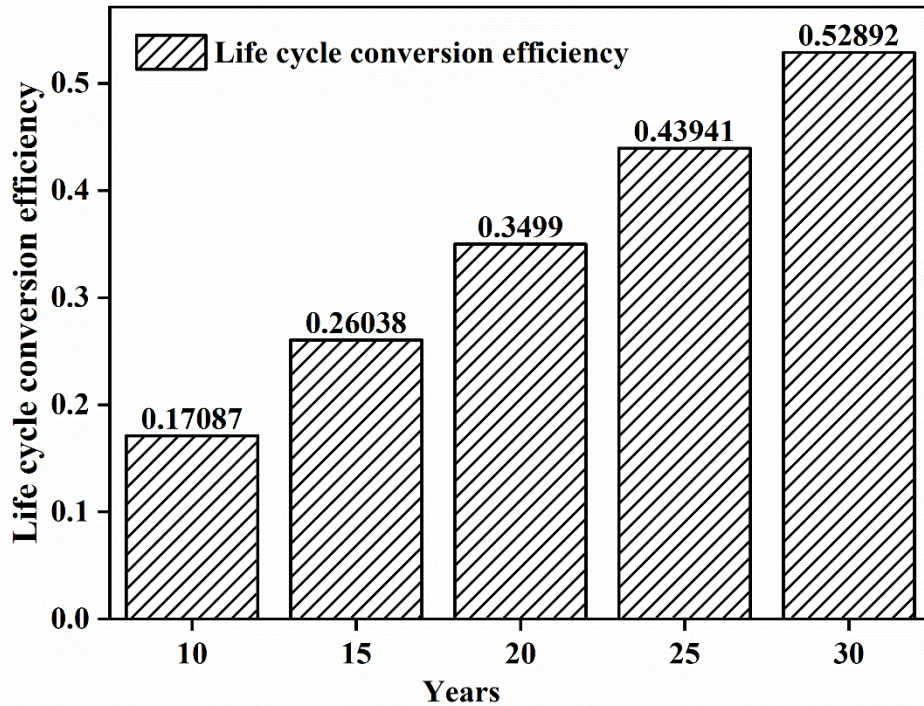


Fig. 13. Yearly variation of life cycle conversion efficiency of the modified still

Table 12. Energy Matrices Analysis

Sl.No	Energy Matrices	Values
1	Energy payback time (Years)	0.45
2	Energy production factor	2.19
3	Life cycle conversion efficiency	0.26

4.5. Water quality test

To estimate the quality of water after desalination, the desalinated water was tested for various quality test parameters. If these quality parameters exceed the safety limits, it may lead to various problems like gas bubbles, heart illness, lung infection, skin disease, laxative effect, somatic damage to the living tissues and neuro affliction in humans [97]. Hence, testing of the water quality after desalination is inevitable. The quality of water before and after desalination was tested at the Environmental and Water Resource Laboratory, VIT University, Vellore, India, and the results are shown in Table 13. The results are compared against the maximum permissible limits of drinking water as per the Bureau of Indian Standards (BIS), New Delhi, India and World Health Organisation (WHO) standards.

Table 13. Comparison of the quality of the water before and after desalination

Water quality parameters	Before desalination	After desalination (conventional still)	After desalination (modified still)	Maximum permissible limits of the drinking water according to BIS [98] and WHO [98,99]
pH	7.7	7.3	6.9	8.5
TDS (ppm)	330	150	51	500
Hardness (mg/L)	254	81	41	200
Dissolved oxygen (%)	78	62	46	60
Fluoride (mg/L)	1.9	0.9	0.3	1.5
Chloride (mg/L)	31.4	19.3	16.2	250
Electrical conductivity ($\mu\text{s/m}$)	637	389	227	1500
Calcium ions (mg/L)	29.7	14.3	8.2	200
Magnesium ions (mg/L)	33	9.4	3.7	200
Sodium ions (mg/L)	372	8	1.5	400
Potassium ions (mg/L)	95	3.7	2	250
Sulphate ions (mg/L)	37	3	1.2	12

596

597 The pH value of the desalinated water was reduced from 7.7 (saline water) to 7.3 for the
598 conventional still and further to 6.9 for the modified still. There was a 5.4% decrease observed
599 in the pH of the modified still as compared to the conventional still. The total dissolved solids
600 in the desalinated water were reduced from 330 ppm to 51 ppm for the modified still
601 contributing an 84.5% decrease. There was a 66% decrease in the TDS observed in the
602 modified still as compared to the conventional still. The hardness of the conventional still is
603 found to be 81 mg/L which is decreased from 254 mg/L (in saline water) contributing to a
604 percentage decrease of 68%. There was a further decrease of 83% observed in the hardness of
605 the desalinated water from the modified still. The percentage of dissolved oxygen in the saline

606 water was 78% and after desalination, the percentage was reduced to 62% and 46% for the
607 desalinated water in the conventional and modified still, respectively contributing a 20.5% and
608 41% decrement from the original value. There was a significant reduction observed in fluoride
609 and chloride ions of the desalinated water (0.3 mg/L and 16.2 mg/L) from modified still as
610 compared to saline water (1.9 mg/L and 31.4 mg/L) corresponding to an 84% and 48% decrease
611 from the initial corresponding values.

612 There was a decrement of 66% and 16% in the fluoride and chloride content of the
613 desalinated water from the modified still, respectively as compared to the conventional still.
614 Similarly, there was a 71%, 88%, 99%, 97% and 96% decrement observed in the calcium,
615 magnesium, sodium, potassium and sulphate ions, respectively in the modified still as
616 compared to the initial value (saline water). Comparing with the conventional still; modified
617 still showed a 42%, 60%, 81%, 45% and 60% decrease in calcium, magnesium, sodium,
618 potassium and sulphate ions, respectively. This decrease in the salt ion has considerably
619 reduced the electrical conductivity of the modified still to 64% and 41% as compared to the
620 saline water and desalinated water in the conventional still.

621 All the test parameters of the desalinated water sample are within the permissible limits as
622 prescribed by the Bureau of Indian Standards (BIS), New Delhi, India and World Health
623 Organisation (WHO) standards [98,99].

624 **5. Future research potential**

625 The literature shows that the integration of high thermal energy storage materials in solar
626 still needs a judicial selection of material. The material should possess high thermal
627 conductivity, latent heat and it should be environmentally benign. For example, the
628 performance of CNT and their derivatives in solar still would be good enough to use in
629 desalination applications. However, CNT is more dangerous to humans because of their
630 noxious nature, dispersion property and toxic characteristics. Hence, the discovery of an eco-
631 friendly energy storage material would be an important breakthrough. Literature suggests that
632 marine biological shells are one such eco-friendly energy storage material. The use of waste
633 biological shells may earn some revenues to countries that rely on seafood. Hence, it is
634 suggested to research the use of such materials like crab shell, sea shell and oyster shell
635 particles [100] as future energy storage materials in desalination applications. In addition,
636 future research should be carried out into optimising the geometrical arrangement of the
637 magnets and the magnetic field strength.

638

639 **6. Conclusion**

640 Experimental investigations on the effects of integrated composite thermal energy storage
641 (both sensible and latent heat) and magnetizing effects (ferrite magnets) were investigated on
642 single slope solar still and compared against the conventional still. Economic analysis, enviro-
643 economic analysis and energy matrices analysis were also performed. Furthermore, the
644 desalinated water quality was also tested and compared with the BIS standards. Based on the
645 experiments, the following conclusions were drawn:

646 The cumulative yield of the modified still was enhanced to 5.5 kg/m²/day from 3.4
647 kg/m²/day (for a conventional still) contributing to a 62% increase in productivity. The evening
648 time productivity (from 17:00 h to 21:00 h) of the modified still increased by 235% due to the
649 addition of integrated energy storage materials and ferrite magnets. The modified still yielded
650 the highest annual productivity of 1375 liters as compared to the conventional still.

651 The cost per liter (CPL) of the purified water from the modified still was \$0.017, which
652 was 3.7% less than the CPL of the purified water from a conventional still. The CPL of
653 freshwater from the modified still was 69% cheaper than the cost of bottled water cost in India.
654 The life cycle conversion efficiency of the modified still was found to be 0.26 and 0.52 at the
655 end of the 15th and 30th years, respectively. There will be 19.8 Tonnes and 40.3 Tonnes of
656 carbon dioxide mitigated from the modified still at the end of the 15th and 30th year, respectively
657 earning a carbon credit of \$198 and \$402. The water quality test reassures that the quality of
658 the desalinated water is under the permissible limits of the Bureau of Indian Standards (BIS).

659 The study concludes that the integration of ferrite magnets, graphite plates and paraffin
660 together in a solar still enhanced the performance of the desalination system from technical,
661 economical, enviro-economic perspectives. Thus, the modified still is recommended as a
662 potential candidate in solar desalination application as it outperforms the conventional still in
663 all the aspects (technical, economical, enviro-economic aspects).

664 **Acknowledgement**

665 The authors duly acknowledge the Vellore Institute of Technology (VIT), Vellore, India for
666 proving the necessary facilities and support for the successful completion of the project.

667 **References**

- 668 [1] A. Boretti, L. Rosa, Reassessing the projections of the World Water Development
669 Report, *Npj Clean Water*. 2 (2019) 1–6. <https://doi.org/10.1038/s41545-019-0039-9>.
670 [2] S. Anvari, O. Mahian, H. Taghavifar, S. Wongwises, U. Desideri, 4E analysis of a
671 modified multigeneration system designed for power, heating/cooling, and water
672 desalination, *Appl. Energy*. 270 (2020) 115107.

- 673 <https://doi.org/10.1016/j.apenergy.2020.115107>.
- 674 [3] A. Colmenar-Santos, E. Palomo-Torrejón, F. Mur-Pérez, E. Rosales-Asensio, Thermal
675 desalination potential with parabolic trough collectors and geothermal energy in the
676 Spanish southeast, *Appl. Energy*. 262 (2020) 114433.
677 <https://doi.org/10.1016/j.apenergy.2019.114433>.
- 678 [4] G. Xiao, X. Wang, M. Ni, F. Wang, W. Zhu, Z. Luo, K. Cen, A review on solar stills
679 for brine desalination, *Appl. Energy*. 103 (2013) 642–652.
680 <https://doi.org/10.1016/j.apenergy.2012.10.029>.
- 681 [5] A. Askalany, E.S. Ali, R.H. Mohammed, A novel cycle for adsorption desalination
682 system with two stages-ejector for higher water production and efficiency,
683 *Desalination*. 496 (2020) 114753. <https://doi.org/10.1016/j.desal.2020.114753>.
- 684 [6] C. Ghenai, D. Kabakebji, I. Douba, A. Yassin, Performance analysis and optimization
685 of hybrid multi-effect distillation adsorption desalination system powered with solar
686 thermal energy for high salinity sea water, *Energy*. 215 (2021) 119212.
687 <https://doi.org/10.1016/j.energy.2020.119212>.
- 688 [7] M.W. Shahzad, M. Burhan, L. Ang, K.C. Ng, Adsorption desalination-Principles,
689 process design, and its hybrids for future sustainable desalination, in: *Emerg. Technol.*
690 *Sustain. Desalin. Handb.*, Elsevier, 2018: pp. 3–34. [https://doi.org/10.1016/B978-0-12-](https://doi.org/10.1016/B978-0-12-815818-0.00001-1)
691 [815818-0.00001-1](https://doi.org/10.1016/B978-0-12-815818-0.00001-1).
- 692 [8] R. Kannan, C. Selvagesan, M. Vignesh, B.R. Babu, M. Fuentes, M. Vivar, I.
693 Skryabin, K. Srithar, Solar still with vapor adsorption basin: Performance analysis,
694 *Renew. Energy*. 62 (2014) 258–264. <https://doi.org/10.1016/j.renene.2013.07.018>.
- 695 [9] A. Al-Ansari, H. Ettouney, H. El-Dessouky, Water-zeolite adsorption heat pump
696 combined with single effect evaporation desalination process, *Renew. Energy*. 24
697 (2001) 91–111. [https://doi.org/10.1016/S0960-1481\(00\)00192-0](https://doi.org/10.1016/S0960-1481(00)00192-0).
- 698 [10] A. Kasaeian, F. Rajaei, W.M. Yan, Osmotic desalination by solar energy: A critical
699 review, *Renew. Energy*. 134 (2019) 1473–1490.
700 <https://doi.org/10.1016/j.renene.2018.09.038>.
- 701 [11] K.C. Ng, K. Thu, Y. Kim, A. Chakraborty, G. Amy, Adsorption desalination: An
702 emerging low-cost thermal desalination method, *Desalination*. 308 (2013) 161–179.
703 <https://doi.org/10.1016/j.desal.2012.07.030>.
- 704 [12] M.A. Alaei Shahmirzadi, S.S. Hosseini, J. Luo, I. Ortiz, Significance, evolution and
705 recent advances in adsorption technology, materials and processes for desalination,
706 water softening and salt removal, *J. Environ. Manage.* 215 (2018) 324–344.
707 <https://doi.org/10.1016/j.jenvman.2018.03.040>.

- 708 [13] A.S. Alsaman, A.A. Askalany, K. Harby, M.S. Ahmed, A state of the art of hybrid
709 adsorption desalination-cooling systems, *Renew. Sustain. Energy Rev.* 58 (2016) 692–
710 703. <https://doi.org/10.1016/j.rser.2015.12.266>.
- 711 [14] N. Ghaffour, T.M. Missimer, G.L. Amy, Technical review and evaluation of the
712 economics of water desalination: Current and future challenges for better water supply
713 sustainability, *Desalination*. 309 (2013) 197–207.
714 <https://doi.org/10.1016/j.desal.2012.10.015>.
- 715 [15] D. Dsilva Winfred Rufuss, S. Iniyan, L. Suganthi, P.A. Davies, T. Akinaga, Analysis
716 of solar still with nanoparticle incorporated phase change material for solar
717 desalination application, in: *ISES Sol. World Congr. 2015*, International Solar Energy
718 Society, Daegu; South Korea, 2015: pp. 1271–1280.
719 <https://doi.org/10.18086/swc.2015.10.44>.
- 720 [16] T. Arunkumar, K. Raj, D. Dsilva Winfred Rufuss, D. Denkenberger, G. Tingting, L.
721 Xuan, R. Velraj, A review of efficient high productivity solar stills, *Renew. Sustain.*
722 *Energy Rev.* 101 (2019) 197–220. <https://doi.org/10.1016/J.RSER.2018.11.013>.
- 723 [17] R. Sathyamurthy, H.J. Kennady, P.K. Nagarajan, A. Ahsan, Factors affecting the
724 performance of triangular pyramid solar still, *Desalination*. 344 (2014) 383–390.
725 <https://doi.org/10.1016/j.desal.2014.04.005>.
- 726 [18] J.A. Andrés-Mañas, L. Roca, A. Ruiz-Aguirre, F.G. Acién, J.D. Gil, G. Zaragoza,
727 Application of solar energy to seawater desalination in a pilot system based on vacuum
728 multi-effect membrane distillation, *Appl. Energy*. 258 (2020) 114068.
729 <https://doi.org/10.1016/j.apenergy.2019.114068>.
- 730 [19] A.A. El-Sebaili, E. El-Bialy, Advanced designs of solar desalination systems: A
731 review, *Renew. Sustain. Energy Rev.* 49 (2015) 1198–1212.
732 <https://doi.org/10.1016/j.rser.2015.04.161>.
- 733 [20] M.R. Karimi Estahbanati, M. Feilizadeh, K. Jafarpur, M. Feilizadeh, M.R. Rahimpour,
734 Experimental investigation of a multi-effect active solar still: The effect of the number
735 of stages, *Appl. Energy*. 137 (2015) 46–55.
736 <https://doi.org/10.1016/j.apenergy.2014.09.082>.
- 737 [21] M.R. Karimi Estahbanati, A. Ahsan, M. Feilizadeh, K. Jafarpur, S.S. Ashrafmansouri,
738 M. Feilizadeh, Theoretical and experimental investigation on internal reflectors in a
739 single-slope solar still, *Appl. Energy*. 165 (2016) 537–547.
740 <https://doi.org/10.1016/j.apenergy.2015.12.047>.
- 741 [22] P. Zanganeh, A.S. Goharrizi, S. Ayatollahi, M. Feilizadeh, H. Dashti, Efficiency
742 improvement of solar stills through wettability alteration of the condensation surface:

- 743 An experimental study, *Appl. Energy*. 268 (2020) 114923.
744 <https://doi.org/10.1016/j.apenergy.2020.114923>.
- 745 [23] S. Shoeibi, N. Rahbar, A. Abedini Esfahlani, H. Kargarsharifabad, Application of
746 simultaneous thermoelectric cooling and heating to improve the performance of a solar
747 still: An experimental study and exergy analysis, *Appl. Energy*. 263 (2020) 114581.
748 <https://doi.org/10.1016/j.apenergy.2020.114581>.
- 749 [24] S.W. Sharshir, G. Peng, L. Wu, F.A. Essa, A.E. Kabeel, N. Yang, The effects of flake
750 graphite nanoparticles, phase change material, and film cooling on the solar still
751 performance, *Appl. Energy*. 191 (2017) 358–366.
752 <https://doi.org/10.1016/j.apenergy.2017.01.067>.
- 753 [25] K.K. Murugavel, S. Sivakumar, J.R. Ahamed, K.K.S.K. Chockalingam, K. Srithar,
754 Single basin double slope solar still with minimum basin depth and energy storing
755 materials, *Appl. Energy*. 87 (2010) 514–523.
756 <https://doi.org/10.1016/j.apenergy.2009.07.023>.
- 757 [26] A. Elfasakhany, Performance assessment and productivity of a simple-type solar still
758 integrated with nanocomposite energy storage system, *Appl. Energy*. 183 (2016) 399–
759 407. <https://doi.org/10.1016/j.apenergy.2016.09.002>.
- 760 [27] D. Dsilva Winfred Rufuss, L. Suganthi, S. Iniyan, P.A. Davies, Effects of
761 nanoparticle-enhanced phase change material (NPCM) on solar still productivity, *J.*
762 *Clean. Prod.* 192 (2018) 9–29. <https://doi.org/10.1016/j.jclepro.2018.04.201>.
- 763 [28] M.S. Sodha, A. Kumar, G.N. Tiwari, R.C. Tyagi, Simple multiple wick solar still:
764 Analysis and performance, *Sol. Energy*. 26 (1981) 127–131.
765 [https://doi.org/10.1016/0038-092X\(81\)90075-X](https://doi.org/10.1016/0038-092X(81)90075-X).
- 766 [29] B.A. Akash, M.S. Mohsen, O. Osta, Y. Elayan, Experimental evaluation of a single-
767 basin solar still using different absorbing materials, *Renew. Energy*. 14 (1998) 307–
768 310. [https://doi.org/10.1016/s0960-1481\(98\)00082-2](https://doi.org/10.1016/s0960-1481(98)00082-2).
- 769 [30] A.S. Nafey, M. Abdelkader, A. Abdelmotalip, A.A. Mabrouk, Solar still productivity
770 enhancement, *Energy Convers. Manag.* 42 (2001) 1401–1408.
771 [https://doi.org/10.1016/S0196-8904\(00\)00107-2](https://doi.org/10.1016/S0196-8904(00)00107-2).
- 772 [31] A.S. Nafey, M. Abdelkader, A. Abdelmotalip, A.A. Mabrouk, Enhancement of solar
773 still productivity using floating perforated black plate, *Energy Convers. Manag.* 43
774 (2002) 937–946. [https://doi.org/10.1016/S0196-8904\(01\)00079-6](https://doi.org/10.1016/S0196-8904(01)00079-6).
- 775 [32] P. Valsaraj, An experimental study on solar distillation in a single slope basin still by
776 surface heating the water mass, *Renew. Energy*. 25 (2002) 607–612.
777 [https://doi.org/10.1016/S0960-1481\(01\)00094-5](https://doi.org/10.1016/S0960-1481(01)00094-5).

- 778 [33] M.M. Naim, M.A. Abd El Kawi, Non-conventional solar stills. Part 1. Non-
779 conventional solar stills with charcoal particles as absorber medium, *Desalination*. 153
780 (2003) 55–64. [https://doi.org/10.1016/S0011-9164\(02\)01093-7](https://doi.org/10.1016/S0011-9164(02)01093-7).
- 781 [34] Z.S. Abdel-Rehim, A. Lasheen, Improving the performance of solar desalination
782 systems, *Renew. Energy*. 30 (2005) 1955–1971.
783 <https://doi.org/10.1016/j.renene.2005.01.008>.
- 784 [35] M. Sakthivel, S. Shanmugasundaram, Effect of energy storage medium (black granite
785 gravel) on the performance of a solar still, *Int. J. Energy Res.* 32 (2008) 68–82.
786 <https://doi.org/10.1002/er.1335>.
- 787 [36] V. Velmurugan, M. Gopalakrishnan, R. Raghu, K. Srithar, Single basin solar still with
788 fin for enhancing productivity, *Energy Convers. Manag.* 49 (2008) 2602–2608.
789 <https://doi.org/10.1016/j.enconman.2008.05.010>.
- 790 [37] V. Velmurugan, C.K. Deenadayalan, H. Vinod, K. Srithar, Desalination of effluent
791 using fin type solar still, *Energy*. 33 (2008) 1719–1727.
792 <https://doi.org/10.1016/j.energy.2008.07.001>.
- 793 [38] V. Velmurugan, K.J. Naveen Kumar, T. Noorul Haq, K. Srithar, Performance analysis
794 in stepped solar still for effluent desalination, *Energy*. 34 (2009) 1179–1186.
795 <https://doi.org/10.1016/j.energy.2009.04.029>.
- 796 [39] A.A. El-Sebaili, S.J. Yaghmour, F.S. Al-Hazmi, A.S. Faidah, F.M. Al-Marzouki, A.A.
797 Al-Ghamdi, Active single basin solar still with a sensible storage medium,
798 *Desalination*. 249 (2009) 699–706. <https://doi.org/10.1016/j.desal.2009.02.060>.
- 799 [40] S. Abdallah, M.M. Abu-Khader, O. Badran, Effect of various absorbing materials on
800 the thermal performance of solar stills, *Desalination*. 242 (2009) 128–137.
801 <https://doi.org/10.1016/j.desal.2008.03.036>.
- 802 [41] F.F. Tabrizi, A.Z. Sharak, Experimental study of an integrated basin solar still with a
803 sandy heat reservoir, *Desalination*. 253 (2010) 195–199.
804 <https://doi.org/10.1016/j.desal.2009.10.003>.
- 805 [42] M. Sakthivel, S. Shanmugasundaram, T. Alwarsamy, An experimental study on a
806 regenerative solar still with energy storage medium - Jute cloth, *Desalination*. 264
807 (2010) 24–31. <https://doi.org/10.1016/j.desal.2010.06.074>.
- 808 [43] H.N. Panchal, Performance analysis of solar still with cow dung cakes and blue metal
809 stones, *Front. Energy*. 9 (2015) 180–186. <https://doi.org/10.1007/s11708-015-0361-y>.
- 810 [44] D.G.H. Samuel, P.K. Nagarajan, R. Sathyamurthy, S.A. El-agouz, E. Kannan,
811 Improving the yield of fresh water in conventional solar still using low cost energy
812 storage material, *Energy Convers. Manag.* 112 (2016) 125–134.

- 813 <https://doi.org/10.1016/j.enconman.2015.12.074>.
- 814 [45] P. Patel, R. Kumar, Comparative Performance Evaluation of Modified Passive Solar
815 Still Using Sensible Heat Storage Material and Increased Frontal Height, *Procedia*
816 *Technol.* 23 (2016) 431–438. <https://doi.org/10.1016/j.protcy.2016.03.047>.
- 817 [46] M. Bhargva, A. Yadav, Experimental investigation of single slope solar still using
818 different wick materials: a comparative study, *J. Phys. Conf. Ser.* 1276 (2019) 012042.
819 <https://doi.org/10.1088/1742-6596/1276/1/012042>.
- 820 [47] H. Panchal, D.K. Patel, P. Patel, Theoretical and experimental performance analysis of
821 sandstones and marble pieces as thermal energy storage materials inside solar stills,
822 *Int. J. Ambient Energy.* 39 (2018) 221–229.
823 <https://doi.org/10.1080/01430750.2017.1298059>.
- 824 [48] K. Rabhi, R. Nciri, F. Nasri, C. Ali, H. Ben Bacha, Experimental performance analysis
825 of a modified single-basin single-slope solar still with pin fins absorber and condenser,
826 *Desalination.* 416 (2017) 86–93. <https://doi.org/10.1016/j.desal.2017.04.023>.
- 827 [49] A.E. Kabeel, S.A. El-Agouz, R. Sathyamurthy, T. Arunkumar, Augmenting the
828 productivity of solar still using jute cloth knitted with sand heat energy storage,
829 *Desalination.* 443 (2018) 122–129. <https://doi.org/10.1016/j.desal.2018.05.026>.
- 830 [50] A.E. Kabeel, M. Abdelgaied, A. Eisa, Enhancing the performance of single basin solar
831 still using high thermal conductivity sensible storage materials, *J. Clean. Prod.* 183
832 (2018) 20–25. <https://doi.org/10.1016/j.jclepro.2018.02.144>.
- 833 [51] P. Dumka, A. Sharma, Y. Kushwah, A.S. Raghav, D.R. Mishra, Performance
834 evaluation of single slope solar still augmented with sand-filled cotton bags, *J. Energy*
835 *Storage.* 25 (2019) 100888. <https://doi.org/10.1016/j.est.2019.100888>.
- 836 [52] A.F. Mohamed, A.A. Hegazi, G.I. Sultan, E.M.S. El-Said, Enhancement of a solar still
837 performance by inclusion the basalt stones as a porous sensible absorber: Experimental
838 study and thermo-economic analysis, *Sol. Energy Mater. Sol. Cells.* 200 (2019)
839 109958. <https://doi.org/10.1016/j.solmat.2019.109958>.
- 840 [53] K. V. Modi, J.G. Modi, Performance of single-slope double-basin solar stills with
841 small pile of wick materials, *Appl. Therm. Eng.* 149 (2019) 723–730.
842 <https://doi.org/10.1016/j.applthermaleng.2018.12.071>.
- 843 [54] T. Arunkumar, D. Murugesan, K. Raj, D. Denkenberger, C. Viswanathan, D. Dsilva
844 Winfred Rufuss, R. Velraj, Effect of nano-coated CuO absorbers with PVA sponges in
845 solar water desalting system, *Appl. Therm. Eng.* 148 (2019) 1416–1424.
846 <https://doi.org/10.1016/j.applthermaleng.2018.10.129>.
- 847 [55] A. Bilal, B. Jamil, N.U. Haque, M.A. Ansari, Investigating the effect of pumice stones

- 848 sensible heat storage on the performance of a solar still, *Groundw. Sustain. Dev.* 9
849 (2019) 100228. <https://doi.org/10.1016/j.gsd.2019.100228>.
- 850 [56] R. Dhivagar, M. Mohanraj, K. Hidouri, Y. Belyayev, Energy, exergy, economic and
851 enviro-economic (4E) analysis of gravel coarse aggregate sensible heat storage-
852 assisted single-slope solar still, *J. Therm. Anal. Calorim.* (2020) 1–20.
853 <https://doi.org/10.1007/s10973-020-09766-w>.
- 854 [57] M.M. Naim, M.A. Abd El Kawi, Non-conventional solar stills. Part 2. Non-
855 conventional solar stills with energy storage element, *Desalination.* 153 (2003) 71–80.
856 [https://doi.org/10.1016/S0011-9164\(02\)01095-0](https://doi.org/10.1016/S0011-9164(02)01095-0).
- 857 [58] A.A.F. Al-hamadani, S.K. Shukla, A. Dwivedi, Experimental Investigation and
858 Thermodynamic Performance Analysis of a Solar Distillation System with PCM
859 Storage: Energy and Exergy, *Distrib. Gener. Altern. Energy J.* 29 (2014) 7–24.
860 <https://doi.org/10.1080/21563306.2014.11442728>.
- 861 [59] M. Asbik, O. Ansari, A. Bah, N. Zari, A. Mimet, H. El-Ghetany, Exergy analysis of
862 solar desalination still combined with heat storage system using phase change material
863 (PCM), *Desalination.* 381 (2016) 26–37. <https://doi.org/10.1016/j.desal.2015.11.031>.
- 864 [60] A.E. Kabeel, M. Abdelgaied, Improving the performance of solar still by using PCM
865 as a thermal storage medium under Egyptian conditions, *Desalination.* 383 (2016) 22–
866 28. <https://doi.org/10.1016/j.desal.2016.01.006>.
- 867 [61] A.E. Kabeel, M. Abdelgaied, M. Mahgoub, The performance of a modified solar still
868 using hot air injection and PCM, *Desalination.* 379 (2016) 102–107.
869 <https://doi.org/10.1016/j.desal.2015.11.007>.
- 870 [62] H. Mousa, A.M. Gujarathi, Modeling and analysis the productivity of solar
871 desalination units with phase change materials, *Renew. Energy.* 95 (2016) 225–232.
872 <https://doi.org/10.1016/j.renene.2016.04.013>.
- 873 [63] V.P. Katekar, S.S. Deshmukh, A review of the use of phase change materials on
874 performance of solar stills, *J. Energy Storage.* 30 (2020) 101398.
875 <https://doi.org/10.1016/j.est.2020.101398>.
- 876 [64] T. Arunkumar, K. Raj, D. Dsilva Winfred Rufuss, D. Denkenberger, G. Tingting, L.
877 Xuan, R. Velraj, A review of efficient high productivity solar stills, *Renew. Sustain.*
878 *Energy Rev.* 101 (2019) 197–220. <https://doi.org/10.1016/j.rser.2018.11.013>.
- 879 [65] D. Dsilva Winfred Rufuss, V. Rajkumar, L. Suganthi, S. Iniyar, Studies on latent heat
880 energy storage (LHES) materials for solar desalination application-focus on material
881 properties, prioritization, selection and future research potential, *Sol. Energy Mater.*
882 *Sol. Cells.* 189 (2019) 149–165. <https://doi.org/10.1016/J.SOLMAT.2018.09.031>.

- 883 [66] D. Dsilva Winfred Rufuss, S. Arulvel, S. Iniyan, L. Suganthi, Numerical study of
884 titanium oxide nanoparticle enhanced energy storage material in solar desalination,
885 Mater. Today Proc. (2020). <https://doi.org/10.1016/j.matpr.2020.06.448>.
- 886 [67] S.M. Shalaby, E. El-Bialy, A.A. El-Sebaii, An experimental investigation of a v-
887 corrugated absorber single-basin solar still using PCM, Desalination. 398 (2016) 247–
888 255. <https://doi.org/10.1016/j.desal.2016.07.042>.
- 889 [68] A.E. Kabeel, G.B. Abdelaziz, E.M.S. El-Said, Experimental investigation of a solar
890 still with composite material heat storage: Energy, exergy and economic analysis, J.
891 Clean. Prod. 231 (2019) 21–34. <https://doi.org/10.1016/j.jclepro.2019.05.200>.
- 892 [69] P. Dumka, Y. Kushwah, A. Sharma, D.R. Mishra, Comparative analysis and
893 experimental evaluation of single slope solar still augmented with permanent magnets
894 and conventional solar still, Desalination. 459 (2019) 34–45.
895 <https://doi.org/10.1016/j.desal.2019.02.012>.
- 896 [70] A.K. Singh, Structure, Synthesis, and Application of Nanoparticles, in: Eng.
897 Nanoparticles, Elsevier, 2016: pp. 19–76. <https://doi.org/10.1016/b978-0-12-801406-6.00002-9>.
- 899 [71] R.G. Keil, L.M. Mayer, Mineral Matrices and Organic Matter, in: Treatise
900 Geochemistry Second Ed., Elsevier Inc., 2013: pp. 337–359.
901 <https://doi.org/10.1016/B978-0-08-095975-7.01024-X>.
- 902 [72] J.S. Lewis, Encyclopedia of Physical Science and Technology (Third Edition), 2003.
- 903 [73] H.M.E. Hisham T. El-Dessouky, Fundamentals of Salt Water Desalination, Elsevier,
904 2002. <https://doi.org/10.1016/b978-0-444-50810-2.x5000-3>.
- 905 [74] H.D. Holland, K.K. Turekian, Treatise on Geochemistry, 2003.
906 <https://doi.org/10.1016/C2009-1-28326-2>.
- 907 [75] J. Feher, Quantitative Human Physiology: An Introduction, in: Am. J. Med. Sci., 2012.
- 908 [76] M. Dubey, D.R. Mishra, Experimental evaluation of double slope solar still augmented
909 with ferrite ring magnets and a black cotton cloth, Int. J. Ambient Energy. (2020) 1–
910 12. <https://doi.org/10.1080/01430750.2020.1722746>.
- 911 [77] R. Dhivagar, M. Mohanraj, Performance improvements of single slope solar still using
912 graphite plate fins and magnets, Environ. Sci. Pollut. Res. (2021) 1–18.
913 <https://doi.org/10.1007/s11356-020-11737-5>.
- 914 [78] A.A. El-Sebaii, A.A. Al-Ghamdi, F.S. Al-Hazmi, A.S. Faidah, Thermal performance
915 of a single basin solar still with PCM as a storage medium, Appl. Energy. 86 (2009)
916 1187–1195. <https://doi.org/10.1016/j.apenergy.2008.10.014>.
- 917 [79] A.E. Kabeel, M.A. Teamah, M. Abdelgaied, G.B. Abdel Aziz, Modified pyramid solar

918 still with v-corrugated absorber plate and PCM as a thermal storage medium, *J. Clean.*
919 *Prod.* 161 (2017) 881–887. <https://doi.org/10.1016/j.jclepro.2017.05.195>.

920 [80] D. Dsilva Winfred Rufuss, S. Iniyan, L. Suganthi, Combined Effect of Heat Storage,
921 Reflective Material, and Additional Heat Source on the Productivity of a Solar Still—
922 Techno-Economic Approach, *J. Test. Eval.* 46 (2018).
923 <https://doi.org/doi.org/10.1520/JTE20170013>.

924 [81] K.N. Knust, D. Hlushkou, U. Tallarek, R.M. Crooks, Electrochemical Desalination for
925 a Sustainable Water Future, *ChemElectroChem.* 1 (2014) 850–857.
926 <https://doi.org/10.1002/celec.201300236>.

927 [82] M. Mehdizadeh Youshanlouei, S. Yekani Motlagh, H. Soltanipour, The effect of
928 magnetic field on the performance improvement of a conventional solar still: a
929 numerical study, *Environ. Sci. Pollut. Res.* (2021) 1–14.
930 <https://doi.org/10.1007/s11356-021-12947-1>.

931 [83] Y. Wang, H. Wei, Z. Li, Effect of magnetic field on the physical properties of water,
932 *Results Phys.* 8 (2018) 262–267. <https://doi.org/10.1016/j.rinp.2017.12.022>.

933 [84] A.A. El-Sebaili, Effect of wind speed on active and passive solar stills, *Energy*
934 *Convers. Manag.* 45 (2004) 1187–1204.
935 <https://doi.org/10.1016/j.enconman.2003.09.036>.

936 [85] T. Arunkumar, D. Denkenberger, A. Ahsan, R. Jayaprakash, The augmentation of
937 distillate yield by using concentrator coupled solar still with phase change material,
938 *Desalination.* 314 (2013) 189–192. <https://doi.org/10.1016/j.desal.2013.01.018>.

939 [86] L. Holysz, A. Szczes, E. Chibowski, Effects of a static magnetic field on water and
940 electrolyte solutions, *J. Colloid Interface Sci.* 316 (2007) 996–1002.
941 <https://doi.org/10.1016/j.jcis.2007.08.026>.

942 [87] S.W. Sharshir, M.A. Eltawil, A.M. Algazzar, R. Sathyamurthy, A.W. Kandeal,
943 Performance enhancement of stepped double slope solar still by using nanoparticles
944 and linen wicks: Energy, exergy and economic analysis, *Appl. Therm. Eng.* 174 (2020)
945 115278. <https://doi.org/10.1016/j.applthermaleng.2020.115278>.

946 [88] H.E.S. Fath, M. El-Samanoudy, K. Fahmy, A. Hassabou, Thermal-economic analysis
947 and comparison between pyramid-shaped and single-slope solar still configurations,
948 *Desalination.* 159 (2003) 69–79. [https://doi.org/10.1016/S0011-9164\(03\)90046-4](https://doi.org/10.1016/S0011-9164(03)90046-4).

949 [89] Chandra Bhushan, The structure and economics of the Indian bottled water industry,
950 *Frontline.* (2006) Volume: 23.
951 <https://doi.org/http://www.frontline.in/static/html/fl2307/stories/20060421006702300>.
952 [htm.](https://doi.org/http://www.frontline.in/static/html/fl2307/stories/20060421006702300)

- 953 [90] P. Joshi, G.N. Tiwari, Energy matrices, exergo-economic and enviro-economic
954 analysis of an active single slope solar still integrated with a heat exchanger: A
955 comparative study, *Desalination*. 443 (2018) 85–98.
956 <https://doi.org/10.1016/j.desal.2018.05.012>.
- 957 [91] K.S. Reddy, H. Sharon, Active multi-effect vertical solar still: Mathematical modeling,
958 performance investigation and enviro-economic analyses, *Desalination*. 395 (2016)
959 99–120. <https://doi.org/10.1016/J.DESAL.2016.05.027>.
- 960 [92] A. Kumar Singh, Samsheer, Material conscious energy matrix and enviro-economic
961 analysis of passive ETC solar still, *Mater. Today Proc.* (2020).
962 <https://doi.org/10.1016/j.matpr.2020.05.117>.
- 963 [93] D.B. Singh, Exergo-economic, enviro-economic and productivity analyses of N
964 identical evacuated tubular collectors integrated double slope solar still, *Appl. Therm.
965 Eng.* 148 (2019) 96–104. <https://doi.org/10.1016/j.applthermaleng.2018.10.127>.
- 966 [94] Ferrite Magnets/Ceramic Magnets Datasheet, (n.d.).
967 [https://www.eclipsemagnetics.com/media/wysiwyg/datasheets/magnet_materials_and_](https://www.eclipsemagnetics.com/media/wysiwyg/datasheets/magnet_materials_and_assemblies/ferrite_magnets-ceramic_magnets_datasheet_v1.pdf)
968 [assemblies/ferrite_magnets-ceramic_magnets_datasheet_v1.pdf](https://www.eclipsemagnetics.com/media/wysiwyg/datasheets/magnet_materials_and_assemblies/ferrite_magnets-ceramic_magnets_datasheet_v1.pdf) (accessed July 24,
969 2020).
- 970 [95] Magnetic properties of ferrite magnets, (n.d.).
971 <https://www.magnetexpert.com/magnetic-properties-of-ferrite-magnets-i699> (accessed
972 July 24, 2020).
- 973 [96] A. Agarwal, R.M. Sarviya, Characterization of Commercial Grade Paraffin wax as
974 Latent Heat Storage material for Solar dryers, in: *Mater. Today Proc.*, Elsevier Ltd,
975 2017: pp. 779–789. <https://doi.org/10.1016/j.matpr.2017.01.086>.
- 976 [97] Nayla Hassan Omer, Water Quality Parameters, in: *Water Qual. Assessments Policy*.
977 IntechOpen., IntechOpen, 2019. <https://doi.org/10.5772/intechopen.89657>.
- 978 [98] T. Arunkumar, K. Raj, M. Chaturvedi, A. Thenmozhi, D. Denkenberger, G. Tingting,
979 A review on distillate water quality parameter analysis in solar still, *Int. J. Ambient
980 Energy*. (2019). <https://doi.org/10.1080/01430750.2019.1587722>.
- 981 [99] A. Shanmugasundharam, G. Kalpana, S.R. Mahapatra, E.R. Sudharson, M.
982 Jayaprakash, Assessment of Groundwater quality in Krishnagiri and Vellore Districts
983 in Tamil Nadu, India, *Appl. Water Sci.* 7 (2017) 1869–1879.
984 <https://doi.org/10.1007/s13201-015-0361-4>.
- 985 [100] S. Arulvel, A. Elayaperumal, M.S. Jagatheeshwaran, Discussion on the feasibility of
986 using proteinized/deproteinized crab shell particles for coating applications: Synthesis
987 and characterization, *J. Environ. Chem. Eng.* 4 (2016) 3891–3899.

988

<https://doi.org/10.1016/j.jece.2016.08.031>.

989